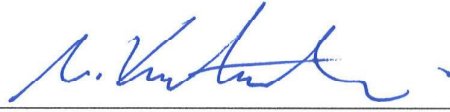# NEURAL NETWORK-BASED ADAPTIVE MYOELECTRIC SIGNAL CLASSIFICATION VIA UTILIZATION OF ENTROPY HISTORY

A THESIS SUBMITTED TO

THE GRADUATE SCHOOL OF

ENGINEERING AND NATURAL SCIENCES

OF ISTANBUL MEDIPOL UNIVERSITY

IN PARTIAL FULFILLMENT OF THE REQUIREMENTS FOR

THE DEGREE OF

MASTER OF SCIENCE

IN

ELECTRICAL-ELECTRONICS ENGINEERING AND CYBER SYSTEMS

By

Kübra Nazlıhan Işık

December, 2017

Neural Network-Based Adaptive Myoelectric Signal Classification via
Utilization of Entropy History
By Kübra Nazlıhan Işık
December, 2017

We certify that we have read this thesis and that in our opinion it is fully adequate,
in scope and in quality, as a thesis for the degree of Master of Science.

_____

Asst. Prof. Dr. Mehmet Kocatürk(Advisor)

_____

Prof. Dr. Bahadır Kürşat Güntürk

_____

Asst. Prof. Dr. Adil Deniz Duru

Approved by the Graduate School of Engineering and Natural Sciences:

_____

Prof. Dr. Talip Alp
Director of the Graduate School of Engineering and Natural Sciences

I hereby declare that all information in this document has been obtained and presented in accordance with academic rules and ethical conduct. I also declare that, as required by these rules and conduct, I have fully cited and referenced all material and results that are not original to this work.

Name, Last Name: KÜBRA NAZLIHAN IŞIK

Signature   :

ABSTRACT

NEURAL NETWORK-BASED ADAPTIVE MYOELECTRIC SIGNAL CLASSIFICATION VIA UTILIZATION OF ENTROPY HISTORY

Kübra Nazlıhan Işık

M.S. in Electrical-Electronics Engineering and Cyber Systems

Advisor: Asst. Prof. Dr. Mehmet Kocatürk

December, 2017

The surface electromyography (sEMG) signals emanating from the remnant forearm muscles of transradial amputees are eligible for controlling robotic prostheses to replace the functions of the lost hand. sEMG pattern recognition (PR) algorithms are utilized in prosthetic decoders to provide intuitive and naturalistic way of control. However, classification accuracy of these algorithms decay over time since the sEMG signal input continuously changes in practice due to the dynamics of muscular contraction and the skin-electrode interface. Our goal in the present study was to develop a computationally efficient classification method that can realize adaptation in an unsupervised manner and improve the performance of the prosthetic hand controllers. To this end, we developed an adaptive, neural-network-based sEMG signal classifier. In the system, the entropy associated with each classification decision is used as a metric to evaluate the confidence level of the predictions. A buffer is implemented into the system to store the history of the entropy and unsupervised learning is realized only when the entropy values associated with the predictions are below a certain confidence level for a certain time period. The present classifier was developed using simulated sEMG signals and its classification accuracy was validated using sEMG signal recordings from two able-bodied subjects performing 5 types of hand gestures. Followed by a supervised training phase using a 25 seconds sEMG signal recording, the average classification accuracy of the classifier for 725 seconds sEMG recordings was 94,5841% and 94,1390% when adaptation is applied and not applied, respectively. The classification accuracy results for the recordings from able-bodied subjects revealed that the present unsupervised, neural network-based adaptation approach is promising for improving the robustness of the prosthetic hand controllers. The present system proposes a computationally efficient solution for the adaptation

problem by utilization of a neural network and online learning strategy. The system stores only the entropy history for a number of latest classifications and performs the adaptation only using the latest sEMG signal input vector.

ÖZET

ENTROPİ GEÇMİŞİNDEN YARARLANARAK SİNİR AĞI TEMELLİ UYARLANABİLİR MİYOELEKTRİK İŞARET SINIFLANDIRMASI

Kübra Nazlıhan Işık

Elektrik-Elektronik Mühendisliği ve Siber Sistemler , Yüksek Lisans

Tez Danışmanı: Yrd. Doç. Dr. Mehmet Kocatürk

Aralık, 2017

Transradiyal amputelerin kalan ön kol kaslarından yayılan yüzeyel elektromiyografi işaretleri(yEMG), kaybedilen elin fonksiyonlarının yerini almak üzere robotik protezlerin kontrolü için kullanılmaya uygundur. Protetik şifre çözücülerde sezgisel ve doğal bir kontrol sağlamak için yEMG örüntü tanıma(ÖT) algoritmalarından faydalanılır. Ancak, şifre çözücüye gelen yEMG işaret girdilerinin adele kasılmaları ve cilt-elektrot arayüzü dinamiğinden kaynaklanan devamlı değişimleri nedeniyle bu algoritmaların sınıflandırma doğruluk değerleri zamanla azalır. Bu tez çalışmasındaki amacımız gözetimsiz uyarlama gerçekleştirebilen ve protez el kontrol birimlerinin performansını arttırabilecek hesapsal olarak verimli bir sınıflandırma yöntemi geliştirmekti. Bu doğrultuda, uyarlanabilir ve sinir ağı temelli bir yEMG işaret sınıflandırıcısı geliştirdik. Her bir sınıflandırma kararı ile ilişkilendirilen entropi, sistemde tahminlerin güvenilirlik seviyelerini değerlendiren bir ölçüt olarak kullanıldı. Entropi geçmişini kaydetmek üzere sistemde bir arabellek tanımlandı ve tahminlerle ilişkilendirilmiş entropi değerleri yalnızca belirli bir zaman aralığında belirli bir güvenilirlik değerinin altında olduğunda gözetimsiz öğrenme gerçekleştirildi. Önerilen sınıflandırıcı benzetilmiş yEMG işaretleri kullanılarak geliştirildi ve sınıflandırma doğruluğu 2 sağlıklı denekten 5 çeşit el hareketinin uygulamaları sırasında kaydedilen yEMG işaret kayıtları kullanılarak doğrulandı. 25 saniyelik bir yEMG işaret kaydı kullanılarak gözetimli eğitim aşaması ardından, 725 saniyelik yEMG işaret kayıtları için sınıflandırıcının uyarlama uygulandığı ve uygulanmadığı durumlar için hesaplanan ortalama genel sınıflandırma doğruluk değerleri sırasıyla 94,5841% ve 94,1390% idi. Sağlıklı deneklerden alınan kayıtlar için elde edilen sınıflandırma doğruluğu sonuçları, bu gözetimsiz, sinir ağı temelli uyarlama yaklaşımının protez el kontrol birimlerinin gürbüzlüğünü arttırma açısından umut

verici olduğunu ortaya çıkarmıştır. Sunulan sistem, uyarlama problemi için sinir ağı ve çevirim içi öğrenme stratejisi kullanarak hesapsal olarak verimli bir çözüm ileri sürmektedir. Sistem yalnızca belirli sayıdaki son sınıflandırma için entropi geçmişi tutmakta ve uyarlamayı yalnızca en son yEMG işaret girdi vektörünü kullanarak gerçekleştirmektedir.

Anahtar sözcükler: EMG, Sinir Ağları, Yüzeyel EMG İşaret Sınıflandırma, EMG İşaret Simulasyonu.

Acknowledgement

I would like to thank to my thesis advisor Mehmet Kocatürk for his great advises and support from the beginning to the end of my master study. I had opportunity to ask any question related to my study, whenever I need. I appreciate for this continuous guidance. Also, I am grateful to my dad for encouraging me to start doing master and to all my family and friends for their support that helped me to keep being in the way.

. . .

Contents

3 NEURAL NETWORK-BASED ADAPTIVE sEMG SIGNAL CLASSIFICATION 49

List of Figures

List of Tables

Chapter 1

INTRODUCTION

The ultimate goal of the surface electromyography (sEMG) signal classification studies is to develop robust and high performance decoders for myoelectric controlled prostheses. A myoelectric controlled prosthesis is an externally powered artificial limb that is controlled by the bio-signals generated from the remnant muscles (skeletal) of the amputees. Improvements in the robotic technology enable the development of prostheses that have multi degrees of freedom (DOF). The number of DOF that a myoelectric controlled prosthesis has indicates its range of motion. Increasing the number of DOF increase the dimensionality of the prosthesis and thus control interfaces should be capable of providing easy and smooth use for the prosthetic users. However, conventional control approaches (e.g. on/off control based on one channel contractions) are inadequate to compensate these multi-dimensionality requirements. In most of the conventional approaches, the user of the prosthesis has to do unnatural co-contractions to transit among several predefined prosthesis motions and to select the motion that the user intended to do. This kind of way of control is cumbersome to the users of the prosthesis which using conventional control approaches that support one DOF(e.g. only simple movements like gripping, open and close) most of the time.

Pattern recognition(PR)-based controllers increase the functionality of the

prostheses. In contrast to the conventional approaches, PR enables to gather more information from the muscles about the movement that the user intended to do. PR algorithms can easily process and distinguish the user signal patterns accordingly. Thus, a PR-based prosthetic user only needs to perform the contractions related with his/her intended movement and algorithm does the rest. Consequently, PR offers more intuitive and natural way of control than the traditional approaches (on/off control based on the contraction detected from single recording channels) do.

Despite the consensus on promising control ability of the PR algorithms, performance reliability of the classifiers has been argued. Non-stationary, time-variant characteristics of the EMG signals are the main reason behind these arguments. Moreover, performance decays can occur in long term (between days) or in short term (within a day, an hour, couple of hour) due to some factors such as user movement pattern variability, electrode shifts, muscle fatigue, electrode-skin contact problems (conductivity changes, humidity, sweating) etc. PR algorithms cannot handle these problems, thus, enhanced algorithms are required to be developed to accommodate the variations in the EMG signals.

Different strategies have been developed to prevent systems from performance degradation. Initial training enhancements to improve classifiers generalization abilities, easier re-training strategies, studies on user adaptation, online training strategies to manage algorithm adaptation can be given as some instances to these solutions that have been developed previously by the other researchers. Recently, adaptive classifier approaches for the sEMG signals have attracted the researchers. Main idea behind the adaptive classifiers is developing algorithms that can adequately update the classifier discriminator parameters and track the changing trends in the sEMG signals in time. Unsupervised adaptation techniques are on demand with reliable and robust online training strategies.

1.1 Literature Overview

Myoelectric controlled prostheses have been developed since 1960s [1]. Mechanical features of the first versions of the prosthetics (e.g. hooks, body powered and on/off controlled myoelectric prosthesis) were easily controllable but limited in the functionality. Multi DOF prostheses were developed to improve the functionality of the artificial limbs. However, control strategies could not fulfill the requirements of the improved mechanical technology. Therefore, PR algorithms have become a prominent solution for the control of multi DOF prosthetics. There is a wide consensus on the PR system contributions but clinical viability of the PR is still argued and could not be tested and proved in all aspects. Numerous studies are conducted to improve PR-based systems reliability.

Since sEMG signal classification studies take part in a multidisciplinary field, that is, intersection of engineering, robotics, neurology and even medicine (e.g. surgical operations like targeted muscle re-innervation(TMR) [2], [3]), the motivations in the studies are widely diversified in the literature. Some of the studies have been concentrated on the development of prosthetic limbs, others focused on the control strategies of the prostheses in the context of software and the hardware developments. sEMG signal classification studies are only one part of the control strategies field.

Effects of the diversity of topics are observed even in this specific research area (EMG signal classification studies). An EMG classification study depends on the numerous conditions and factors by its own. Most of the factors in different conditions that may affect the performance of the classifier are separately investigated. The factors that may affect the EMG signal classification studies can be categorized into; data acquisition techniques, user himself/herself, data processing and classification techniques (These categories include numerous parameters that may affect the performance).

In the data acquisition point of view; different data acquisition configuration settings, conducted movements, movement performing variations (i.e. isotonic

(muscle length changes), isometric (no muscle length changes), transient (dynamic, short and burst), steady-state (constant force) contractions) are investigated. The number of the channels that is required to develop an EMG data acquisition setup has argued [4] and it was demonstrated that, using more than 2 channels substantially improve the classification performance of the systems.

The impact of the limb position [5], electrode size [6], electrode location and orientation on the limb were the other topics that the researchers have been studied on for the performance improvements. A training strategy has been applied to prevent the system from accuracy degradations that may be caused from the electrode displacements [7]. It was called "grouping training" in the study and it was done by augmenting initial training data with possible electrode displacement patterns. In another study, same strategy has been used with a small difference to resolve performance decay problem that is caused by different limb positions. In this strategy, in addition to the EMG patterns limb accelerometer sensor data was added to the initial training data aiming to improve generalization ability of the classifier by teaching the classifier possible pattern variations of each classes [8]. Moreover, in a recent study, a prostheses control strategy robust to limb position was proposed by utilizing sparse representations [9]. Inter-electrode distance and different electrode configuration effects on the system performance has been studied too [10]. Studies that has been conducted in the literature shows the variety of the factors that may affect performance of the sEMG signal classification studies.

Different muscular structures that the individuals have make the user himself/herself the most important factor for the classification studies due to their specific physiological and anatomical properties. The user has been described in a study as "source of the greatest variability" [11]. In this study, a virtual reality environment (VRE) was provided to the user to ease the system training that has been developed (real time controlling of the virtual prosthesis with a classifier). It demonstrates that subject could learn the classifier dynamics and performed more repeatable movements after spending some time using the virtual prosthesis. At the end, user performed more repeatable movements and performance of the system improved. Moreover, the performance results of the system which is

reported in [12] revealed the user adaptation ability in the performance.

Actual prosthetic users are amputees obviously. Their residual muscles are capable of generating EMG signals and these signals can be used to control robotic wrist and hand movements. The user characteristics vary more than non-disabled individuals. Individuals amputated from their forearms have different name according to their amputation levels such as below elbow and above elbow amputations are called transradial and transhumeral respectively. In the majority of the studies, amputee and intact individuals have been involved in the experiments together. On the other hand, only non-disabled subjects have participated in some studies. Similarities between those subject groups (amputees vs. non-amputees) in terms of training abilities and system usage error rates/performances has been reported in numerous studies [13]. Generally, performance similarity between non-disabled and transradial amputees is higher than transhumeral amputees. Because transradial amputees have more and sufficient number of remnant muscles than transhumeral amputees. Even for high effort required complex motions like finger muscle activities could be classified and classification accuracy results comparisons between non-disabled and transradial amputees revealed similar performance within two groups [14]. In a study, high error rates have been reported for the transradial amputees initially but the error rate has been reduced after user training over time and similar performance with the non-disabled individuals has been achieved by the amputees accordingly [15]. The reason behind the initially high error rates is that the transradial amputee has short limb that make the remnant muscle hard to produce intended movements. However, the amputee can learn to use his/her remnant muscles efficiently by training to control the prosthetic and the error rate is decreased resultantly. These findings show that, the studies involving only able bodied individuals are acceptable to test developed schemes for the future prosthetic applications.

Data preprocessing methods are one of the most important factors that may affect classification performance. Some of the preprocessing methods that have been applied in the literature can be listed as noise filtering, dimensionality reduction techniques (e.g. principal component analysis before classification [15]) and time window length [16]. Time window length is one of the important parameter

5

in the preprocessing methods. Sufficient window length should be determined. Since features of the current sEMG signal will be extracted from these windows, length of the windows should be long enough to represent main characteristics of a class. However, it should not be too long that can be led to late classifier decisions. The length of the time window should be short enough to have a classifier that make fast classification decisions during use of the prosthesis.

1.1.1 Surface Electromyography(SEMG) Signals Classification

sEMG signals are acquired during performing real limb motions. The data gathered from multiple muscles enable classifiers to capture muscle synergy patterns and maps data patterns into motion labels [17]. Classification algorithms are the interfaces between human and the prosthetics in this manner. However the decisions of the classifiers are not mechanical output of the prosthetics. Functional assessments of the PR systems on the prosthesis have to be carried out additionally [18].

Feature extraction is the first and important step of the classification problems. EMG signals are divided into temporal segments and time domain features are extracted from each of these segments which are called time windows. Many different features and feature groups are evaluated and alternative feature sets have been sought to find best performing classifier in the literature [19], [20]. Feature extraction process should suit the real time control requirements of the prosthetic devices. Time domain features such as mean absolute value (MAV) and waveform length (WL) are suitable to be used in real time [16] control due to easy computations [21] and stability [22] to the changes over time. Besides, similar performance results have been reported when the time domain features and the complex features such as discrete wavelet are compared [23]. Therefore, time domain features are most commonly used features in the previous studies.

Most of the classification algorithms have been studied including non-linear

(e.g. multi layer perceptron (MLP)) and linear ones (e.g. linear discriminant analysis (LDA)) in the literature. High classification accuracies are reported mostly above 90% accuracies for both classifier types in general. Non-linear classifiers offer better classification accuracy than linear ones [23] for the EMG signal due to its unpredictable, complex, non-stationary nature. However, LDA is the mostly used classifier among the classifiers in the literature. The reasons behind the use of the LDA were indicated in most of the studies as being widely used and its easy implementation. It is applied conventionally [16] and in different expanded versions (e.g. LDA with multiple binary classifications [18]) as well.

In addition to LDA classifier, other classifiers have been used in the literature are support vector machine (SVM) [24], hidden markov models (HMM) [25], gaussian mixture model(GMM) [26], k-nearest neighbor (knn) [27] etc.. High accuracy results have been reported in most of the studies. Different classifier and feature combinations have been used to discriminate sEMG signals for each study. High accuracy results that are attained by different classifiers can be interpreted as inconsistency for the literature. But the factors such as data acquisition tools, data processing methods, movements that are conducted by the subjects and the subjects who are involving to the experiments vary among studies basically. Therefore, performance results that have been reported for each study in the literature may be unique in nature [28]. It is hard to make comparative interpretations among studies.

Nevertheless, it is possible to find an eligible classifier and feature combination according to the acquired data patterns. The evaluation criteria for selecting classifier and feature combinations can be the applicability of the online training (learning) procedure to the classifier and both features and classifiers should be satisfying the real time constraints. These are important properties to prevent systems from performance degradations that may be caused by stochastic nature of the sEMG signals. The algorithm should be capable of adapting the changes that may occur in the sEMG signal patterns and algorithm should be upgraded properly.

1.1.2 Adaptive Classification Approaches

sEMG signals are complex and unpredictable signals due to their non-stationary and time-variant nature. When other external factors (e.g. sweat, muscle fatigue, electrode displacements, humidity, changes in the quality of the signal etc.) are involved in the process, signals become harder to discriminate over time. Especially the conventional PR algorithms fail to accommodate sEMG signals dynamics over time. In conventional PR algorithms, only one initial training phase is executed to compute the parameters of the classifier. These parameters are used to make classification decisions and do not change during classification phase. When the signal patterns start to change and differentiate from the initial training data patterns, previously calculated parameters (during initial training) cannot handle the process and start to deteriorate accuracy of the classifier by making wrong decisions for new encountered exemplars.

Previous efforts that have been made to improve the performance of the sEMG classification studies mostly concentrate on the pre processes before the classification phase. The strategies such as applying proper data acquisition techniques, determination of the best feature and classifier combinations provide high classification accuracies. However, these strategies only offer high performance in a certain time, with a limited data without considering effects on the system performance that may caused over time.

More recently, adaptive classifiers have taken interests of the researchers since they can be a solution for the performance degradations over time. Adaptive classifiers are developed to accommodate the changes and aim to recover possible system performance degradations. An adaptive scheme can detect the abnormalities in the classifier performance and adjust the classifier parameters accordingly. As an example, Thakor et al. (2012) developed an adaptive algorithm which is based on LDA, detects deteriorations of the signal and categorize them into different types as slow changes and fast changes by using entropy calculations [29]. Different update strategies have been applied for each type of deterioration in the study.

In order to develop a good adaptive classifier, computationally efficient update strategies should be developed. It should ensure that the classifier applicable when it makes decisions in real time, real time classification and training constraints should be considered. Robust, reliable and unsupervised adaptation strategies [30] are on demand currently [31]. Within this context, crucial properties that an adaptive classifier should satisfy can be listed as:

- Less update frequency [32], [33]: algorithms need to have a metric to adjust the update frequency.

- Easy implementation of online training [32].

- Low computational load for update strategy: computationally intense updating algorithms should be avoided [32], [19].

- Valid online training data [19]: This issue is important especially for developing unsupervised adaptive strategies. Since target classes are unknown during classification, choosing new samples to update existing classifier can be cumbersome. It is easier to do in supervised strategies, since input-label pairs are known even during classification phase.

- Size of the online training data: small amount of data required to reduce the time required to complete the online training and also to reduce computational load.

Sensinger et al. (2009) have evaluated different types of online training data modifications including supervised and unsupervised methods by utilizing entropy [34]. The results that have been obtained in this study revealed that supervised approaches provide better performance due to target classes are known. But application of a supervised scheme is cumbersome to the user, since the user should give feedback frequently to provide correct labels to the system. Nishikawa et al. (2001) is one of the example for supervised training strategy [35]. They have proposed real time learning scheme utilizing feed-forward neural network as classifier and back propagation (BP) algorithm as training strategy in their

studies [35], [36]. User judgements control the learning process to teach system new motions and adapt the system to a specific user. Moreover, if the user does not satisfy the system performance, he/she can re-teach movement set to the network. BP learning helps network to update its weights in a supervised way by using 'teacher signals' sent by the user to label the signal patterns for the current movement data. When the user wants to teach new motion to the system, lastly calculated feature vectors are added to the training data set and training occurs using this updated training data set. A root mean squared (RMS) threshold was used to stop the training process (all data points in the training data should satisfy the condition).

As it is previously mentioned, low computational load should be satisfied for the update strategy. Easy and computationally efficient update methods have been proposed for the LDA classifier in this manner. In order to retrain the LDA classifier, covariance matrices are required to be recalculated. However, recalculation of the covariance matrices during classification task is computationally intensive and it is a problem for the real time use of the prosthetic device. In one of the study[37], to simplify the recalculation of the covariance matrix, instead of calculating entire covariance matrix for each update step, only small modifications have been made on the covariance matrix like in another study [38]. The study has been proposed to prevent the classification performance from degradations based on detecting abnormal activities on the EMG signals. When the abnormalities are detected in the sEMG channels, signals that are gathered from those channels not included into the samples that will be classified. Similarly, related information about the abnormal activity detected EMG channels have been extracted from the covariance matrices at the same time to track the changes in the signals (basically to adapt). Residual parts of the covariance matrices have been used to classify EMG patterns, thus this procedure simplifies and speeds up the retraining process.

It has been revealed that, unsupervised solutions are required to develop self adaptive approaches. Chen et al. (2013) offers a unsupervised way of update strategy utilizing labels of the decision outputs of the classifier, LDA that has been used in the study[38]. Classifier parameter, covariance matrix, has been

iteratively updated, after every decision output using classified labels. Similarly, in another study update frequency of the classifier is in every test sample classification [39]. However, it is an intensive work and may led wrong classifications due to the only criteria for labeling the upcoming samples the classifier decision itself. There is no controlling mechanism to valid classifier outputs. Therefore, confidence metrics are used as an evaluative metric for deciding on the data that is used to update the classifier parameters. In the study of Amsuss et al. (2014), an ANN has been used as a confidence metric [30]. The network has been employed as a self assessment mechanism for the LDA classifier outputs and corrects the classifier decisions accordingly.

Fukuda et al. has been made one of the greatest contribution to the literature belonging to adaptive EMG classifier studies [40]. Combination of feed-forward neural network and GMM discrimination functions creates a probabilistic neural network which has been employed to classify sEMG signal patterns. Time-series of the sEMG signals have been as the inputs of the network. Adaptation scheme updates network parameters by using back-propagation (BP) learning and apply suspension rule that output the network to no motion. Entropy has been used as confidence metric that decide whether an update is required or not. If calculated entropy during classification is under a predetermined threshold, network updates the weights by utilizing BP learning. Before retraining the network, training data set is modified by adding the last sample to the training data set and removing oldest data sample from the existing data set. Since this adaptation scheme uses all the training data to apply retraining and update network parameters, it is a time consuming task. Substantial amount of time is required to complete training data convergence [41]. It is not certainly explained in the study that update of the network weights occurs with the previously calculated weights or the weights are randomly initialized for every new update step. If it is randomly initialized, convergence of the training data samples can take more time [42], [43], [44], [45].

1.1.3 Artificial Neural Networks as EMG Signal Classifiers

It is well known that, artificial neural networks (ANN) can classify any kind of distributed (linear or non-linear) data. A well constructed network makes non-linear mappings between inputs and output classes through network training strategies. Back-propagation learning algorithm is a well-known and mostly used training strategy in the sEMG ANN classification studies. The algorithm updates the network weights using each data point in the training data set. Basically error between desired output and actual output of the network are propagated to the network from output to input in the BP training. The training continues until network learns to discriminate all the training data examples correctly.

In one of the study, Baspinar et al. (2013) have been compared classifiers Gaussian mixture model (GMM) and ANN with different network structures in terms of classification rates as classifier performance metric [46]. An ANN with 20 neurons in hidden layer outperformed the GMM classifier. In another study, ANN and LDA classifiers comparison has been made in the cases of electrode shift [6]. It has found that, LDA has better generalization ability than ANN in the cases of electrode shifts.

First real time ANN based sEMG signal classification study has been performed by Hudgins et al. (1993) [47]. Time domain features (i.e. MAV, MAV Slope, zero crossing (ZC), slope sign changes (SSC), WL) have been used in the study as features. In the study, a 3 layered feed-forward back-propagation neural network (BPN) have been constructed. Classification scheme has an adaptation unit to modify network weights for the possible small variations of the features. When error rate of the network is under a predetermined error rate threshold, re-training occurs starting from the last updated network weights until the error rate becomes under desired value. This study offers a supervised adaptation scheme, since target class labels are given to the adaptation unit during classification to calculate error rates and to track performance degradations.

Tenore et al. (2009) have used ANN to discriminate separate finger movements [14]. The best time domain features and neural network combination were argued. The results of the study show that, WL gave the best performance in terms of classification accuracy among the time domain features for the classifier ANN. No adaptation procedure has been applied in some of the NN-based classification studies. Only optimal network structures has been sought to gain high classification accuracies considering the network complexity [48], [49].

In another three layered feed-forward NN based study [50], training is realized by utilizing BP. The existing training (learning) data has been modified and the network retrained by using the new training data inputs (samples) during classification. Training data modification has been made by utillizing three different methods that the study proposed: selective addition, automatic addition, and automatic elimination. Alternative online training methods has been developed such as: a neural network architecture uses varying learning rate has been constructed to improve and speed up BPN learning during classification [51].

1.2 Objectives of the Thesis

As it is mentioned in the previous sections, sEMG signals are non-stationary and time-variant biological signals. PR algorithms offer high classification accuracies but reliability problems are occurred over time due to the unpredictable nature of the sEMG signals. The main objective of the present thesis was to develop a robust, reliable and unsupervised adaptive sEMG signal classification method that can be used in the prosthetic limb controllers and can be a solution for the recent reliability problems that the PR algorithms suffer from. In this sense, an adaptive classifier was developed using neural networks and an unsupervised way of adaptation is implemented using entropy.

The online training strategy of the present algorithm is superior to the other training strategies with its computationally efficient and reliable updating procedure. The update occurs only in the predetermined time intervals and if some

specific conditions are met. This strategy substantially improves the robustness of the adaptive classifier.

1.3   Outline of the Thesis

At the beginning of Chapter 2, a brief explanation about sEMG signal generation in terms of physiological aspects is given. Subsequently, the properties of the sEMG model that has been used in the thesis are disclosed. sEMG signals corresponding to different movements are generated using this model. The generated sEMG signals are later distorted to simulate the conditions in which classifier adaptations are required. The simulated and distorted signals are presented in the following sections. The neural network-based sEMG classifier is described and its adaptation capability is studied using the simulated sEMG signals. The classification performance of the classifier is shown and discussed at the end of the chapter.

In chapter 3, an improved version of the adaptive classifier is introduced. It is improved by utilizing entropy history of the neural network. The classification and adaptation performance of the classifier is studied using real sEMG signals recorded from able-bodied subjects.

Lastly in chapter 4, thesis concludes with summary of the entire thesis. Advantages and disadvantages of the developed system are presented. The main contributions of the present study and possible future improvements are identified.

Chapter 2

SURFACE EMG SIGNAL SIMULATIONS and NEURAL NETWORK-BASED sEMG SIGNAL CLASSIFICATION

2.1 Introduction

Electromyography signals (EMG) are electrical activities that originate in the skeletal muscles. They are generated during muscle contractions as a result of chemical, electrical and mechanical reactions. EMG signals can be recorded over the skin by using surface electrodes. Electrode records the average potential underneath the electrode[52] namely pick-up area [6] and surface electromyography signals (sEMG) are constituted.

EMG signal generation mechanism in a physiological and anatomical extent has drawn attention for decades. In order to improve our understanding about the EMG signals, EMG models have been developed. The models mainly aim to study the effects of the parameters on the generated signal properties (e.g.

waveform, amplitude) and subsequently establish relationship between the signal and the physiological and anatomical properties of the muscle [53], [54]. On the other hand, the models provide variable controllability [52], thus they can be used to assess the developed algorithms.

EMG models are simply based on mathematical derivations of the signals. One of the earliest mathematical descriptions has been made by Plonsey [55], [56], Rosenfalck and Andreasan [57]. The smallest source of the EMG signals, fiber action potentials, have been generated by using these mathematical solutions [58], [59].

The sEMG signals that are detected over the skin can be simulated by utilizing the mathematical derivations of the EMG models. Within this context, a simple sEMG model is generated in the present thesis. Generated model dynamics are based on Merletti EMG model [60] and roughly encompass main functional features of real sEMG signals. Merletti model is expanded into multi MUAP model that simulates sEMG signals. In the present study, it is attempted to generate two-channel bipolar electrode recordings. Different signal combinations of two channels are created to simulate distinct movement patterns. Simulated signals are distorted with a variety of distortion levels. Finally, resulted signals are classified using an adaptive neural network classifier.

The aims of the present chapter can be listed as:

- constructing a basic sEMG model(construction of a realistic model is out of scope of this study),

- creating distinguishable movement signal patterns,

- investigating the performance of the adaptive classifier we developed for distorted sEMG signals(simulations with known parameters provide sufficient interpretations to see the algorithms [61] accuracy and robustness prior to the tests using experimenter sEMG signal recordings).

In this chapter, basics about an EMG signal generation during muscle contractions will be presented concisely before the sEMG model explanations. Afterwards, properties of sEMG model, simulated signals and distorted versions of the simulated signals will be given. Brief explanation about the first version of the adaptive neural network classifier will be made (expanded version of it will be introduced in the next chapter). Distorted signal classification results will be compared between the cases in which adaptive and non adaptive classifier are used. Finally, the chapter concludes with the classifier results and discussions.

2.2 Methods

2.2.1 sEMG Signal Simulation of Movements

2.2.1.1 Theoretical background

An EMG signal simply originates in skeletal muscles. A skeletal muscle is composed of motor units (MU) and each MU is composed of variety number of fibers. Number of MUs and fibers of each MU may vary among muscles [53] .

The smallest portion of an EMG signal is initiated in neuromuscular junctions (NMJ) of the fibers. Neuromuscular junction is the location where a motor neuron and a fiber is connected. The motor command received from the motor neuron activates the fiber and the other fibers that are coordinated from same motor neuron through their NMJs. A motor neuron and the fibers it innervates constitute the smallest functional unit of a muscle which is called motor unit (MU). Activation of each fiber of the MU discharges action potentials and forms motor unit action potential (MUAP) accordingly [62], [63], [53].

Contraction of a muscle is initiated by the activation of single MU but this activation creates weak contraction. Thus, contributions of more MUs increase the force generated by the muscle. To sustain a contraction, MUs are repeatedly

activated [53]. Potentials that are generated during this activation interval constitute MUAP trains (MUAPT) [64]. Occurrence frequency namely firing rate of each MUAP in a MUAPT may change in time according to number of active MUs.

Created action potentials from active fibers of MUs linearly contribute to the electric field spatially and temporally in and around a muscle [65]. An EMG surface electrode is located on the skin in a place in the vicinity of the related muscle can be recorded effectively. The recorded signal consists of the superposition of MUAPs generated under the detection area of the electrode basically. Resultant signal that is recorded by the electrode is called surface electromyogram (sEMG) signal.

2.2.1.2   About the model in general

In the present study, Merletti's EMG model [60] is used to simulate sEMG signals. The model constitutes a sEMG signal by potential generated at intracellular level to extracellular level. In the study, only single MU action potential and its current created on the surface have been simulated. Several assumptions have been made to simplify implementation of the model (i.e. tissue between surface and the source(s)(signal generation points like fiber NMJ)) is assumed as homogeneous and anisotropic conducting semispace limited by a plane (skin surface) of infinite extent. Despite the simplifications, model is sufficient to generate sEMG signals to investigate effects of the parameters such as conduction velocity, depth of the fiber in a muscle and different recording electrode configuration on the shape of the generated MUAP [52].

In the present study, two-channel differential (bipolar recording configuration) sEMG signals are generated using this model. Unlike Merletti, more than one MUAP are calculated to constitute the sEMG signal. Additionally, two different signal sources are simulated. It is intended to create 4 different sEMG channel signal combinations that can be distinguishable in the classification experiments. Different parameters have been used for each channel, i.e. number of MU and

conduction velocity of the fiber. The details about the movement generation will
be given in the following sections.

2.2.1.3   Equations of the model and their relation with the theory

Main components of the model is shown in the diagram which is represented in
Figure 2.1.
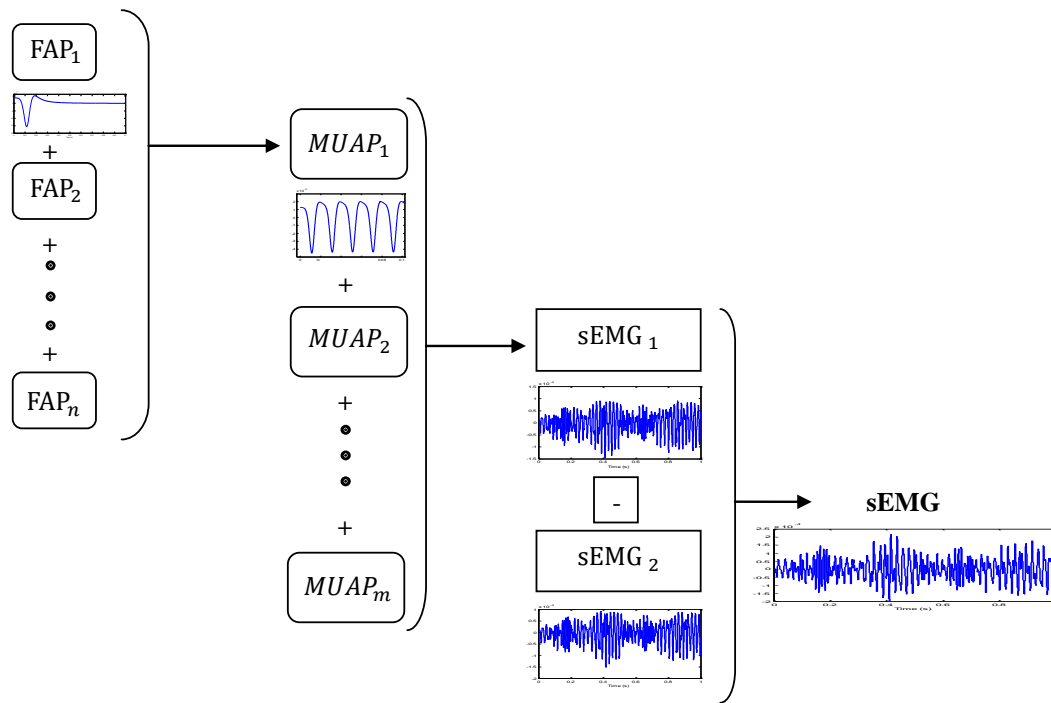
Figure 2.1: Architecture of the sEMG model. Basic operations of generating a
sEMG signal that simulate the signals obtained from one channel are shown in
the figure. Signal graphs show 1 second signal simulations (FAP: Fiber Action
Potential, MUAP: Motor Unit Action Potential, SEMG: Surface EMG).

The diagram shows the main operations of the constructed model to generate
the sEMG signal. Basically, superposition of several fiber action potentials con-
stitute a motor unit action potential (e.g. MUAP1) as illustrated in Figure 2.1.
Other MUAPs which involve the constitution of sEMG1 signal are created by
contribution of different number of fibers for each MUAP. $sEMG_1$ and $sEMG_2$
represents the signals of first and second electrodes of a channel respectively. In

order to simulate bipolar electrode configuration recordings, signals of these two electrodes are subtracted from each other to form the resultant signal $sEMG$.

2.2.1.4   Fiber action potential in intracellular field

Simulation of a sEMG signal starts from the intracellular level. As it is mentioned previously, a single fiber action potential initiate at the NMJ of the fiber where the activation command received. Generated action potentials at the NMJ (locates in the middle of the fiber approximately) of a fiber propagate along the fiber length towards two opposite directions longitudinally with a constant velocity and extinguish at the tendon ends of the fiber [66]. This propagation mechanism is attempted to simulate in the current model. It is assumed that potential has triphasic shape. Three poles are calculated symmetrically located both side of the NMJ which is denoted as z within this manner using current distribution equation 2.2 which is derived from the fiber action potential equation 2.1. Consequently 6 poles are obtained for each instant current positions, 3 poles of each action potential propagate along the fiber length by the equation $c_v t$ in time t in opposite directions.

Intracellular action potential of a fiber is denoted by the mathematical expression:

$$V_m(z) = A(\Lambda z)^3 e^{-\Lambda z} - B. \tag{2.1}$$

and second derivative of the fiber potential is the current distribution [52] which is calculated as:

$$I_m = CA\Lambda^2(\Lambda z)[6 - 6\Lambda z + (\Lambda z)^2]e^{-\Lambda z} \tag{2.2}$$

where Λ is scaling factor in mm^{-1}, C is a proportionality constant, z is distance along the fiber length (reference point is NMJ point of the fiber) depends on the

conduction velocity and time, calculated as $c_v t$. A and B are action and resting state potential constants respectively.

2.2.1.5   Fiber action potential in extracellular field

Tissue between the source (active fiber cell NMJ point inside the muscle) and the skin affects the signal recorded over the skin. For the sake of simplicity, tissue effects such as low pass filtering are neglected in the model. It is not aimed to create a realistic model in the present study as it is mentioned previously.

Since a sEMG model is indented to generate, calculated potentials in the intracellular level are transformed to the skin level. Thus, action potential of a fiber that is detected over the surface of the skin is formulated in the model as:

$$V = \frac{1}{2\pi\sigma_r} \sum \frac{P_i}{\sqrt{(h^2)K_a + (z_i - z)^2}} \tag{2.3}$$

σ_r is electric conductivity (S/mm) along fiber radius r, P_i is current value of the pole i that is calculated using equation 2.2, h is depth of the fiber underneath the skin, K_a is anisotropy ratio(ratio between conductivities in the longitudinal and perpendicular directions) that equals to σ_z/σ_r, σ_z and σ_r are electric conductivities along z and r directions, Z_i is distance between electrode location and the NMJ along fiber length parallel to the skin surface.

2.2.1.6   Motor unit action potential

As it is mentioned previously, a MUAP is the superposition of fiber action potentials which are involved in the electrode detection field. Different number of fibers are defined and MUAPs that is generated on the surface of the skin are calculated using the equation 2.3 for each MU. MUAP shape and the amplitude highly depends on the factors like distance between detection site and origin of the signal [61], number of fibers and their firing rates and conduction velocity etc.

These effects are clearly observed during simulation calculations. For instance, there is an inverse relationship between the duration time of an action potential and its conduction velocity, as it has been revealed in De Lucas study [67]. Thus, same conduction velocities (c_v) are determined for each fiber of a MU but conduction velocity for each MU is different.

2.2.1.7 Surface EMG signal simulation

After calculating a single MUAP, there were three more steps that should be taken to achieve the intended model solution. These steps can be listed as: electrode signal simulation, bipolar recording simulation and final sEMG signal simulation. Resulted sEMG signal represents the signal which is recorded from one channel. Movement simulations have been made accordingly by changing the parameters (e.g. firing rate, number of fibers, and conduction velocity of the fiber) of the involved fibers for each channel.

A duration time was determined for the signal simulations (20 seconds signals are generated). MUAPs are generated repeatedly by varying firing rates. Firing rate of the MUAPs was reduced by two (2) for the following MUAPs that will be involved into the signal that is recorded from one electrode. This process simply constitutes MUAP train (MUAPT) in the predetermined time interval. Number of occurrences of one MUAP in the MUAPT varies according to the firing rate, electrode-source distance and time interval. Additionally, electrode location values of the fibers are increased incrementally to simulate action potentials move in time (generating times of the single fiber action potentials differ), simply to generate MUAPTs. Consequently, linear summation of the MUAPTs constitutes the sEMG signal which is recorded from one of the electrodes in the bipolar electrode pair [52].

Only difference between the bipolar electrode signals is having different z_a (electrode position) values, all the other parameters are exactly same for each sEMGs (these are sEMG1 and sEMG2 signals as represented in Figure 2.1). Two different electrode locations were determined and the distance between the

electrode pairs was 2 cm approximately and same for all movement simulations. It can be considered as second electrode recordings are different representation of the first electrode signals shifted in time. However they are not exactly same, due to different initial electrode locations resultant signal vary in time (differ in shape and amplitude).

To simulate different movements, the parameters like number of MUs, number of fibers of each MU and the conduction velocities of the fibers for each MU are adjusted differently for each channel. These parameter adjustments enable the simulation of distinct movement signals in terms of shape and amplitude for each channel signals. [68]

2.2.1.8   Assumptions of the model

The action potential of a fiber is generated as a tripole. It is assumed that fibers of the motor units are distributed parallel to the skin. All the fibers are assumed to be in the same depth and have same length and radius. The diameters of the fibers are neglected. Fibers are considered as line sources. The difference between firing rate of the MUs and the distance between two bipolar electrodes were same for each generated sEMG signal. Electrode spatial extent is restricted only to parallel direction to the skin, along to fiber length. Tissue effect between the electrode and the source is neglected. Different conduction velocities, number of MUs and fibers of each MU are determined to constitute different sEMG signals in terms of shape and amplitude.

2.2.2   Distorted Signal Simulation

Amplitudes of the simulated signals are changed gradually (increased and decreased) to create distortions like in the conditions sweating or misconduct issues between skin and the electrode. Loose conduct between the skin and the electrodes may lead to decrease and sweating may lead to increase on the amplitude of the EMG signals. Classification and adaptation performances are investigated

during variations of the signal.

Different amount of distortion levels have been applied to all of the previously simulated movement signals. Distorted signal patterns are created for each simulated movement signal. Distortion only applied to the signals of the one channel of the channel pair.

Distorted signals are simulated as amplitude changes on the signals using the equation[69]:

$$y = (1 \pm d)y \tag{2.4}$$

where y is the signal which is intended to distort, d is the rate of distortion. $-$ and $+$ signs are for the adjustment of the distortion level. $-$ decrease and $+$ increase the amplitude of the signal y.

2.2.3 Neural Network Adaptation

General architecture of the system is shown in Figure 2.3. An adaptive neural network classification algorithm is developed to adapt to the variations in the signals. Training and test data sets are constructed by extracting features from the simulated signals. A simple three layered feed-forward neural network used as the main classifier that calculate initial outputs. Neural network that is used in the present study is consisted of 8 input, 4 hidden, 4 output layer neurons. Structure of the network is illustrated in Figure 2.2.

Calculated outputs are not accepted as classifier decisions directly. An evaluative confidence metric, entropy, is used to control classifier outputs. Entropy can be calculated using Equation 3.1(in Chapter 3). Interpretations that made by entropy calculation basically based on the argument; high entropy means low confidence and low entropy means high confidence. Entropy thresholds are determined according to this argument. It is crucial to define a suitable confident zone
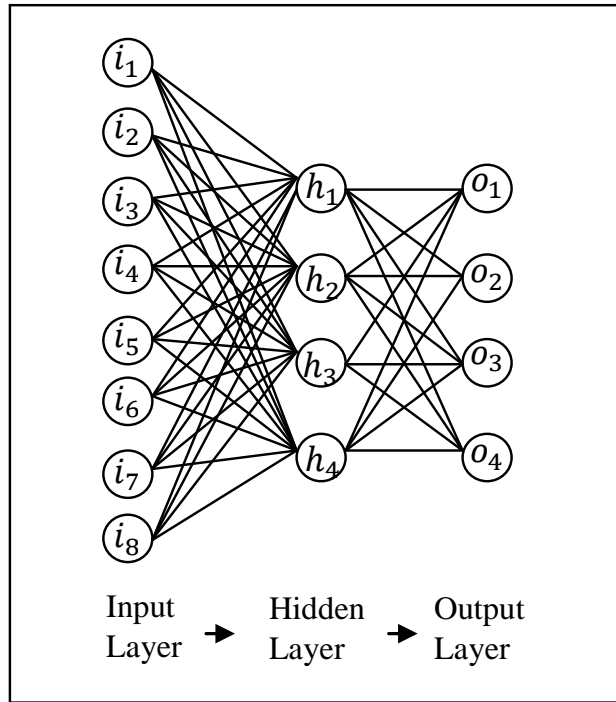
Figure 2.2: Structure of the neural network.

where adaptation can be applicable. It is assumed that entropy increases but no wrong classifications occur in these threshold intervals. Thresholds are defined empirically after several evaluations made on the classification results. Simultaneous classifier decision results and entropy calculation plots made easier to spot increased but correctly classified entropy values. Thus, entropy value of the network output is controlled immediately to check the difference between calculated entropy and the threshold intervals. If the calculated entropy value fits in the threshold intervals classifier is retrained by this recent input samples, otherwise classifier makes the decision without any retraining process (retraining was held by applying back propagation online learning and only the last sample used to update network weights that can be used for the next classifications). This is the first version of our adaptive neural network, details about the classifier will be given and expanded version of the classifier will be introduced in the next chapter (Chapter 3).
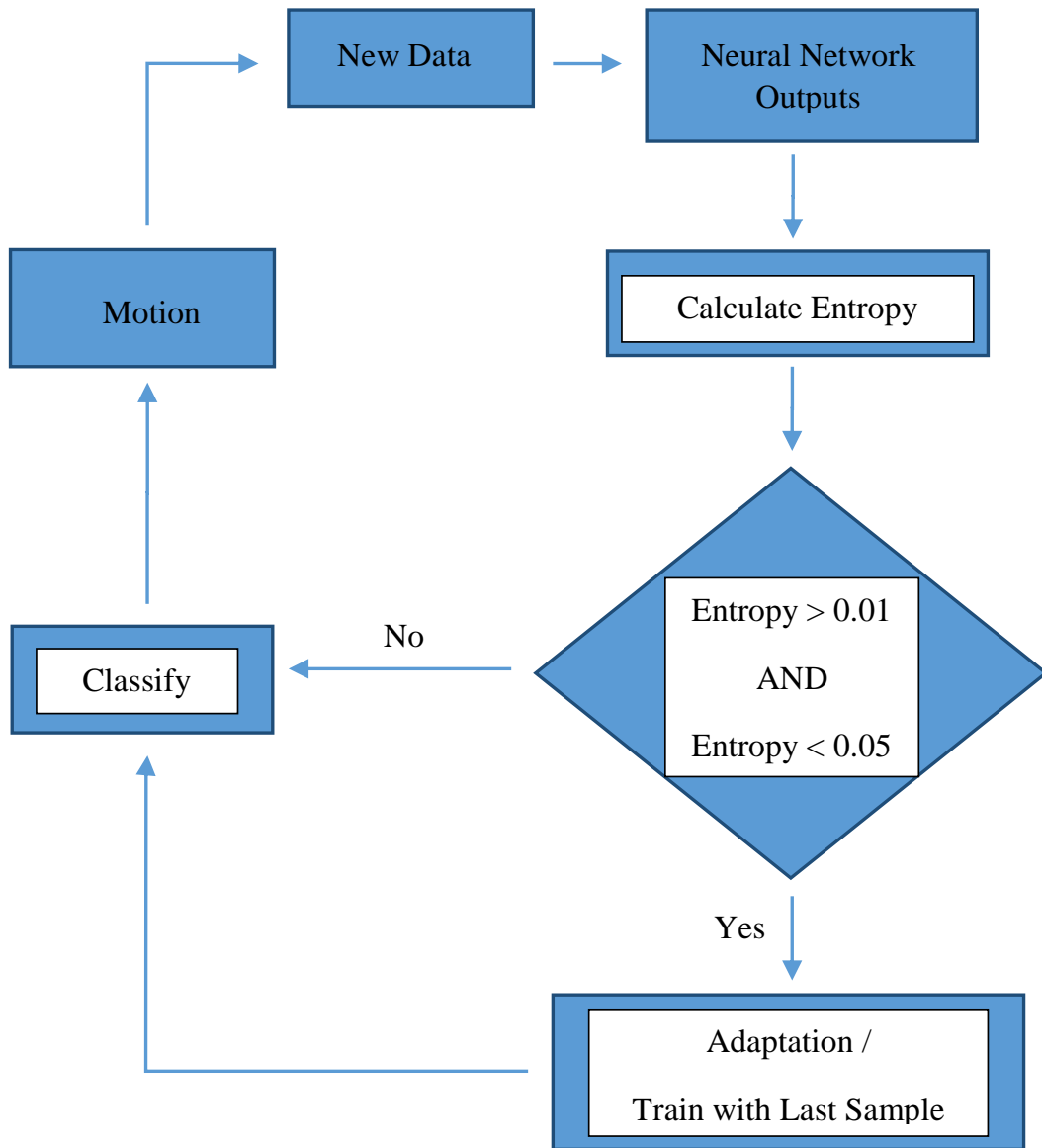
Figure 2.3: Structure of the adaptive neural network.

2.3 Results

2.3.1 Simulated Signals

20 seconds signals are simulated for each movement. Constant parameters were determined as: A = 96mV is action potential, B = 90mV resting state potential and radial conductivity; σ_r =0,330 [60].

2.3.1.1 Wrist extension movement simulation

Wrist extension movement signal simulation is plotted in Figure 2.4.
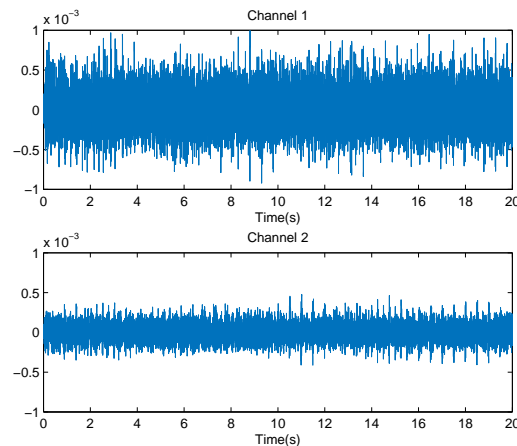

Figure 2.4: Simulated signal of movement wrist extension.

Parameters of the simulated signal wrist extension:

Channel 1:

Conduction velocities of each MU respectively = [6 6.5 7 7 7.2 7.5 7.5 8 8 8 8]m/s. Number of fiber of each MU = 10.

Channel 2:

Conduction velocities of each MU respectively = [4 4.4 5 5 5.5 5.5]m/s. Number of fiber of each MU = 5.

2.3.1.2 Wrist flexion movement simulation

Wrist flexion movement signal simulation is plotted in Figure 2.5.

Figure 2.5: Simulated signal of movement wrist flexion.

Parameters of the simulated signal wrist flexion:

Channel 1:

Conduction velocities of each MU respectively = [4 4 4 5 5 5.5]m/s. Number of fiber of each MU = 5.

Channel 2:

Conduction velocities of each MU respectively = [6.5 6.5 6.5 6.5 7 7 7 7.2 8 8 8]m/s. Number of fiber of each MU = 10.

2.3.1.3 Hand close movement simulation

Hand close movement signal simulation is plotted in Figure 2.6.

Parameters of the simulated signal hand close:

Channel 1:

Conduction velocities of each MU respectively = [4 4 5 5 5.5 6 7 7.2 7.5 8 8 8]m/s. Number of fiber of each MU = 10.

Channel 2:

Figure 2.6: Simulated signal of movement hand close.

Conduction velocities of each MU respectively = [4 4.4 5 5 5.5 5.5 6.5 6.5 7 8 8]m/s. Number of fiber of each MU = 10.

2.3.1.4 Hand open movement simulation

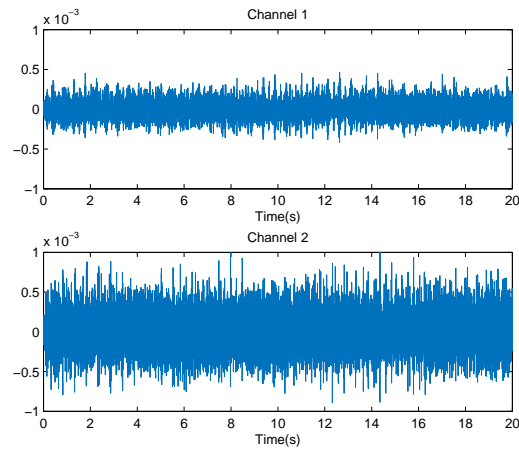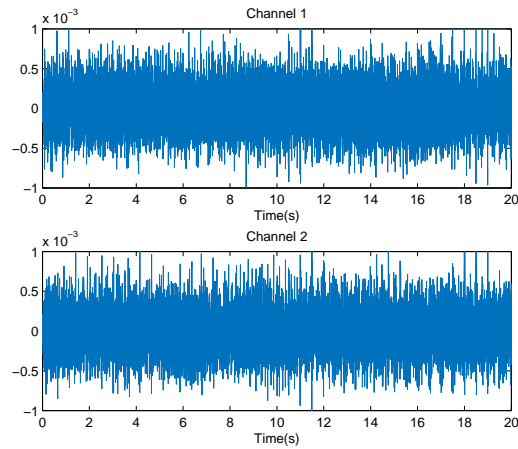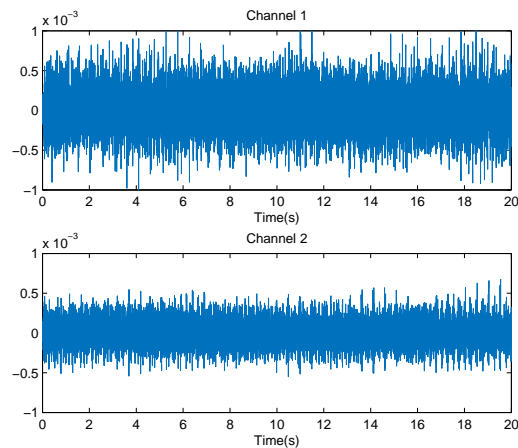Hand open movement signal simulation is plotted in Figure 2.7.

Figure 2.7: Simulated signal of movement hand open.

Parameters of the simulated signal hand open:
Channel 1:

Conduction velocities of each MU respectively = [4 4 5 5 6 7 7 7.2 7.5 8 8]m/s.
Number of fiber of each MU = 10.

Channel 2:

Conduction velocities of each MU respectively = [4 5 5 5.5 5.5 6 6]m/s. Number
of fiber of each MU = 7.

2.3.2 Adaptation Results for Distorted Signals

2.3.2.1 Distorted signals

First 10 seconds of the simulated 20-seconds sEMG signal is distorted in differ-
ent levels and appended consecutively to create three different distorted signal
arrangements (DT1-3). 10 seconds of the signal corresponds to 200 samples of
the simulated patterns. Distortion is applied only on the signals corresponding
to the first channel in each movement.

Three different signal arrangements (DT1-3) are made for each movement sig-
nal pattern. Distortion arrangement types are described below for each differently
arranged signal patterns:

Distortion type 1 (DT1): Starting with 10 seconds of the simulated undis-
torted signal patterns, 5% distortion rate is applied to the same undistorted
signal and appended at end of the undistorted signal. This process is continued
incrementing distortion rate by 5% until distortion rate reaches 50%. After that,
distortion rate that is applied on the simulated signal start to decrease by 5%
until reaching 0% distortion rate -it will be the same undistorted signal that was
given to the neural network at the beginning. The same undistorted 10 seconds
signal patterns are appended to at the end of the signal arrangement (DT1) three
times. As an instance, distorted and rearranged wrist flexion movement signal
patterns appended according to the DT1 distortion type is shown in Figure 2.8.

Distortion type 2 (DT2): 10 seconds undistorted simulated signal patterns
are located at the beginning of the signal arrangement. Distortion rate that the
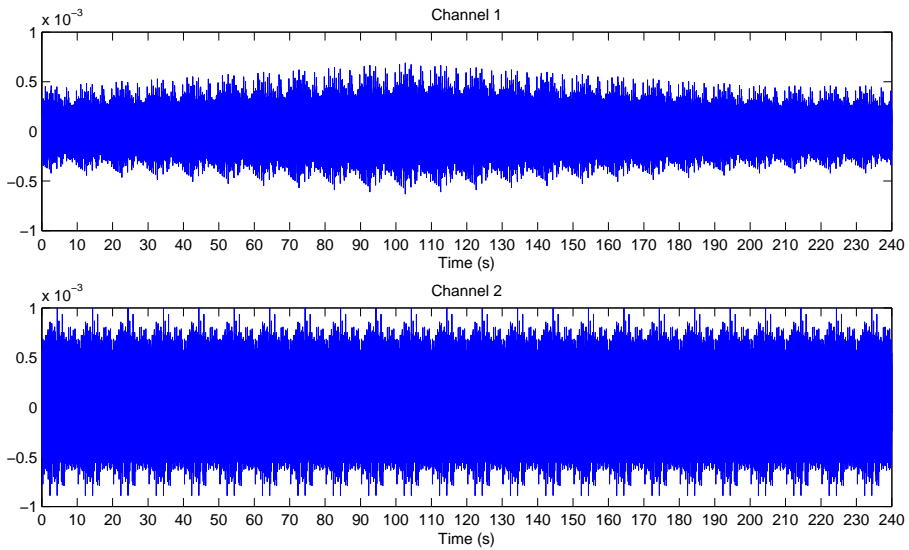
Figure 2.8: Distorted wrist flexion movement signal which is arranged by DT1

same 10 seconds undistorted signal exposed starts to increase by 5%. Increasing distortion rate is continued until distortion rate reaches 50%. It is the maximum level of the distortion, after that distortion rate start to decrease gradually by 5% until reaching 0% distortion rate. Each distorted signal is appended next to each other. 10 seconds undistorted signal patterns are added at the end of the distorted signals several times (i.e. 20 times). As an instance, distorted and rearranged wrist flexion movement signal patterns appended according to the DT2 distortion type is shown in Figure 2.9.

Figure 2.9: Distorted wrist flexion movement signal which is arranged by DT2

Distortion type 3 (DT3): Undistorted 10 seconds signals are appended at

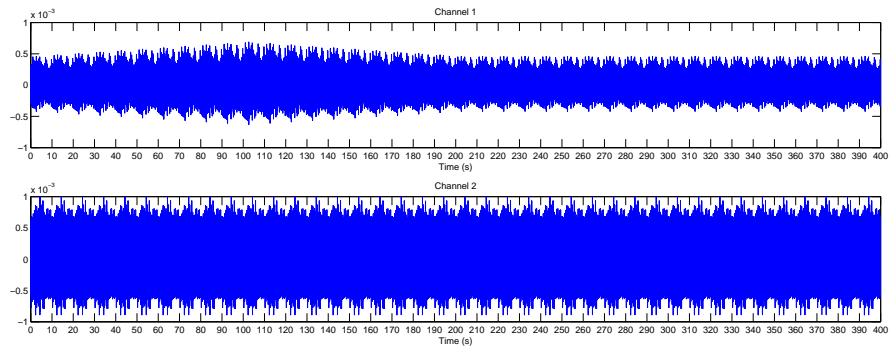the beginning of the signal arrangement 20 times. Afterwards, the undistorted signals start to distort by 5% distortion rate. Distortion rate is incrementally increased by 5% until reaching 50% distortion rate like the other distortion types (DT1 and DT2). Distortion rate of the signals exposed gradually decreased by 5% until 5% distortion rate is reached. As an instance, distorted and rearranged wrist flexion signal movement signal patterns appended according to the DT3 distortion type is shown in Figure 2.10.
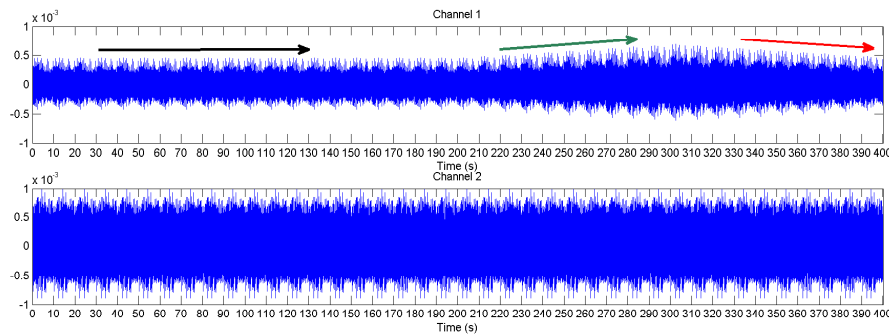
Figure 2.10: Distorted wrist flexion movement signal which is arranged by DT3

2.3.2.2 Adaptive neural network

Neural network that is used in the present study is consisted from 8 input, 4 hidden and 4 output layer neurons as it is mentioned in the methods section. Learning rate that is used during training of the classifier to obtain initial weights and during adaptation process was same (i.e. 0.15). Training of the constructed neural network is continued until all movement patterns are correctly classified (after 16374 epochs training stopped). Training and test data are constructed by extracting root mean square (RMS) and wavelength (WL) features separately from all time windows of simulated signals. Movement data patterns (extracted feature vectors from time windows) are fed to the neural network in the following order: wrist flexion, hand close, wrist extension and hand open. Upper entropy threshold is 0.05 and lower threshold is 0.01. Adaptation is applied when the entropy that is calculated from the decision outputs is in this threshold interval as shown in Figure 2.3.

32

Classification accuracy results for each distortion type (DT1-DT3) and for each movement are shown in Figures 2.11, 2.12, 2.13, 2.14. The results of the movement signal patterns are represented in the same order as the movement patterns are fed to the neural network. Every 10 seconds, the signal classification accuracy is calculated using Equation 3.3 and shown below in graphs.

Results for DT1:

The results for DT1 signal classification are shown in the graphs for each movement with the same order as the movement patterns were fed to the classifier. Figures 2.11, 2.12, 2.13, 2.14 present wrist flexion, hand close, wrist extension and hand open movements classification accuracy results, respectively.

Results for DT2:

The results for DT2 signal classification are shown in the graphs for each movement with the same order as the movement patterns were fed to the classifier. Figure 2.15 presents wrist flexion results, 2.16 presents hand close results, 2.17 presents wrist extension results, 2.18 presents hand open results, respectively.

Results for DT3:

The results for DT3 signal classification are shown in the graphs for each movement with the same order as the movement patterns were fed to the classifier. Figure 2.19 presents wrist flexion results, 2.20 presents hand close results, 2.21 presents wrist extension results, 2.22 presents hand open results, respectively.

Figure 2.11: The classification accuracy results for type 1 distorted (DT1) for wrist flexion movement. The classification results where no adaptation is applied are shown in graphs A, B and C. A) The output class labels of the network for each data point(sample). Class labels are represented by numbers 1 to 4 for wrist flexion, wrist extension, hand close, hand open movements, respectively. Green stars and red stars represent true and wrong classified samples by the classifier, respectively. B) Entropy after each decision of the classifier. C) Classification accuracy calculations shown by black stars for every 200 samples.

Classification results where adaptation is applied are shown in graphs D & E. D) Entropy after each classification (adaptation is applied during classification). E) Classification accuracy calculations for every 200 samples shown by black stars. The samples where the adaptation applied marked by blue vertical triangles.

2.4   Discussion

Distortion Type 1(DT1) Results:

Wrist flexion movement patterns are the first patterns that are fed to the network. The classification accuracy results for type 1 distorted signals for the movement are shown in Figure 2.11. The highest distortion level corresponds to the samples where the highest entropy values are observed (Figure 2.11B). Meanwhile, the patterns where the lowest accuracies (Figure 2.11C) are observed have the highest entropy value (Figure 2.11B). The increase and the decrease in the entropy trends can be clearly seen from Figure 2.11B. When the entropy graphs are compared for the cases in which adaptation is applied (Figure 2.11D) and not applied (Figure 2.11B), it can be said that after applying adaptation, entropy is substantially decreased as expected. As a result of decrease in the entropy, increases are observed in the classification accuracies (Figure 2.11D).

No decrease is observed in the classification accuracy for the next upcoming patterns (hand close movement patterns), when the accuracy results of the first samples of the movement in the cases where adaptation is applied and not applied are compared which are shown in Figure 2.12C and E. It shows that previously applied adaptations (in the wrist flexion movement patterns) did not lead to any difference on the classification accuracy. Nevertheless, adaptation points are seen at the first samples of the movement due to the increased entropy. The number of adaptation points are gradually increased for the next samples of the movement as a result of the gradual distortion increases. When adaptation is not applied, accuracy starts to decrease after 1000 samples, it corresponds to the samples where 25% distortion rate is applied, decrease continues until reaching 50% distortion rate, lowest accuracy is observed as a result of 50% distortion in Figure 2.12B. In addition, in the classification accuracy results where the adaptation applied (Figure 2.12E), starting from the samples where classification accuracy start to decrease (25% distortion rate) in the case of no adaptation applied (Figure 2.12C), it is observed that adaptation algorithm starts to recover distortion effects on the accuracy. It is valid even for the cases where highest distortion rate is reached, significant enhancement on the accuracy can be seen in Figure 2.12E when it is compared with the accuracy results where no adaptation applied (Figure 2.12C). Since it is the second time of the algorithm comes across with
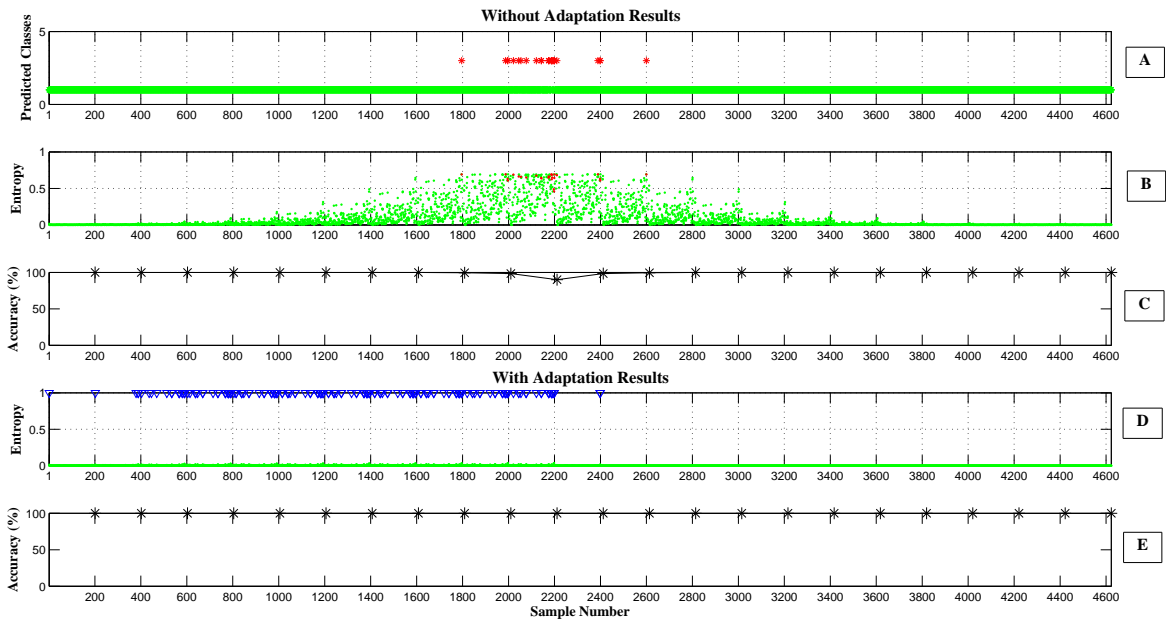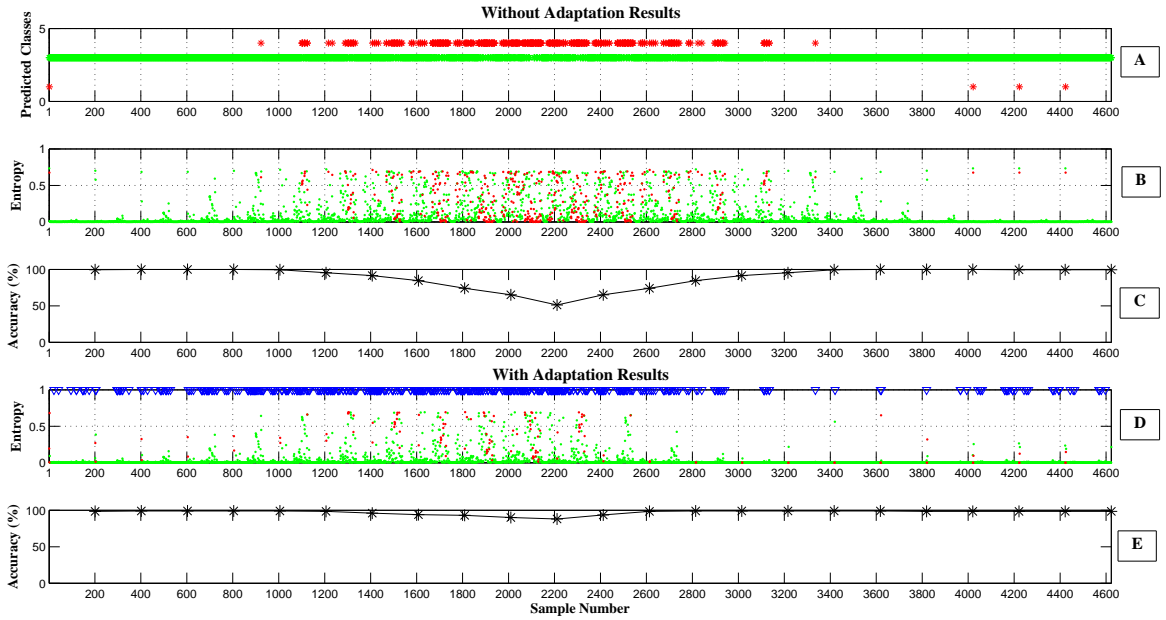
Figure 2.12: The classification accuracy results for type 1 distorted (DT1) for hand close movement. The classification results where no adaptation is applied are shown in graphs A, B and C. A) The output class labels of the network for each data point(sample). Class labels are represented by numbers 1 to 4 for wrist flexion, wrist extension, hand close, hand open movements, respectively. Green stars and red stars represent true and wrong classified samples by the classifier, respectively. B) Entropy after each decision of the classifier. C) Classification accuracy calculations shown by black stars for every 200 samples.

Classification results where adaptation is applied are shown in graphs D & E. D) Entropy after each classification (adaptation is applied during classification). E) Classification accuracy calculations for every 200 samples shown by black stars. The samples where the adaptation applied marked by blue vertical triangles.

the same distorted patterns, faster recovery is observed than the previous distorted patterns recovery in the accuracy results where the adaptation applied for the next upcoming patterns (Figure 2.12E). The number of samples where the adaptation applied start to decrease after 2600 samples. It can be explained by those samples does not require any further adaptation due to 100% classification

accuracy is reached and entropy is in the intended level (smaller than 0.01) for those samples.

In Figure 2.13, wrist extension movement classification accuracy results are shown. It can be said that, wrist extension movement did not affected by the distortion like the other movement patterns affected. In the classification accuracy results where the adaptation is not applied (Figure 2.13C), 100% accuracy is observed for all the sample groups (every 200 samples), there is no any decrease are observed in the accuracy due to the distortion. When accuracy results in the cases adaptation is applied and not applied are compared, decrease in the accuracy of the first sample group of the movement where adaptation is applied can be related with the previous class adaptations (hand close movement samples). Changes in the weights may be not suitable for the new class patterns/samples (wrist extension) and algorithm may not adapt this rapid changes and cause to decrease the classification accuracy. However, it is seen in the graph that it does not take too long (Figure 2.13E). After 200 samples algorithm recover the classification accuracy and reach the same classification accuracy values (Figure 2.13E) with the accuracy results where no adaptation is applied (Figure 2.13C) quickly.

In the results of the last inputs of the network (hand open movement patterns), no decreases are observed in the accuracies of the first sample groups of the movement when the accuracy results in the cases where adaptation is applied and not applied are compared for graphs are shown in Figure 2.14C and E. Hand open movement patterns are the patterns which are highly affected by the distortion as it can be seen from the dramatic decreases in the classification accuracy results in the case where no adaptation is applied (Figure 2.14C). For example, when the distortion rate reached 40%, algorithm did not classify any patterns correctly (0% accuracy). In the case of adaptation is applied, significant increases in the accuracy are observed when it is compared with the accuracy results where no adaptation is applied. Especially, when the distortion level start to decreases in the accuracy results where no adaptation is applied (Figure 2.14C) , high amount of recovery is observed from 0% (without adaptation) to 100% (with adaptation) when it is compared with the accuracy where adaptation is applied (Figure 2.14E). It reveals that the adaptation algorithm has good recovery performance even in
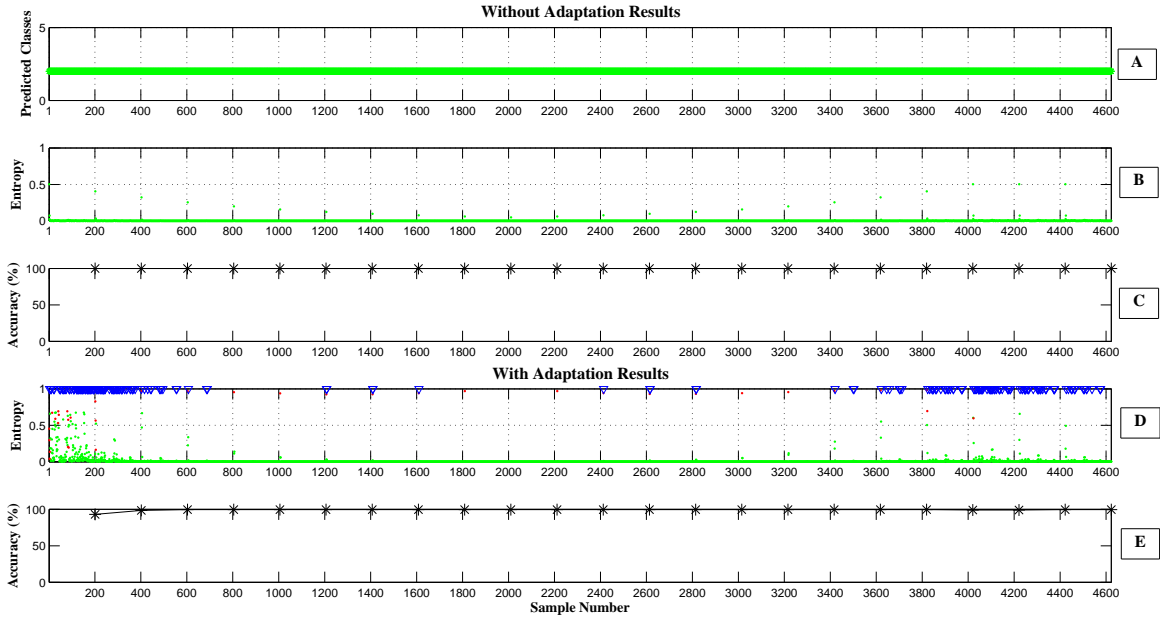
the high amount of distortion levels.

Figure 2.13: The classification accuracy results for type 1 distorted (DT1) for wrist extension movement. The classification results where no adaptation is applied are shown in graphs A, B and C. A) The output class labels of the network for each data point(sample). Class labels are represented by numbers 1 to 4 for wrist flexion, wrist extension, hand close, hand open movements, respectively. Green stars and red stars represent true and wrong classified samples by the classifier, respectively. B) Entropy after each decision of the classifier. C) Classification accuracy calculations shown by black stars for every 200 samples. Classification results where adaptation is applied are shown in graphs D & E. D) Entropy after each classification (adaptation is applied during classification). E) Classification accuracy calculations for every 200 samples shown by black stars. The samples where the adaptation applied marked by blue vertical triangles.

Distortion Type 2 (DT2) Results:

In the DT2 type of distorted signal arrangement, same patterns that belong to same class are fed to the network subsequently a couple of times at the end of the

38

distorted signal patterns. The reason for this kind of arrangement is to see if the algorithm can adapt when different class patterns are fed to the network right after the patterns belonging to the same class. Thus, the patterns belonging to the same class are fed to the network 20 times at the end of the distorted signals (once a time corresponds to 200 samples of the class patterns where the accuracy is calculated). However, no significant amount of decreases are observed on the classification accuracies at the transition times when new class patterns (different from the previous class patterns) are fed to the network (for instance, Figures 2.16E and 2.17E). Also, similar accuracies are observed for the signals corresponding to distortion type 1 (DT1). It shows that the algorithm has the ability to prevent the classifier from over training. It may be achieved by choosing proper entropy thresholds that prevents algorithm from excessive adaptation.

Distortion Type 3 (DT3) Results:

It is observed that changing the order of the distorted patterns in the signal arrangements do not have any effect on the classification accuracy results. The classifier can transited among distorted signal patterns without any significant loss in the accuracy and adapted to the new situations easily.

Consequently, small variations and changes in the signal patterns can be recovered by the adaptation algorithm. Even in the cases when the highest amount of distortion is applied (50%) adaptation performance is still valid. It shows that adaptation algorithm that is developed in this chapter is capable of adapting new patterns for different situations. The results based on utilization of simulated sEMG signals in this chapter reveal that our algorithm can be further applied for classification of experimental sEMG signal recordings from subjects.

Figure 2.14: The classification accuracy results for type 1 distorted (DT1) for hand open movement. The classification results where no adaptation is applied are shown in graphs A, B and C. A) The output class labels of the network for each data point(sample). Class labels are represented by numbers 1 to 4 for wrist flexion, wrist extension, hand close, hand open movements, respectively. Green stars and red stars represent true and wrong classified samples by the classifier, respectively. B) Entropy after each decision of the classifier. C) Classification accuracy calculations shown by black stars for every 200 samples.

Classification results where adaptation is applied are shown in graphs D & E. D) Entropy after each classification (adaptation is applied during classification). E) Classification accuracy calculations for every 200 samples shown by black stars. The samples where the adaptation applied marked by blue vertical triangles.

Figure 2.15: The classification accuracy results for type 2 distorted (DT2) for wrist flexion movement. The classification results where no adaptation is applied are shown in graphs A, B and C. A) The output class labels of the network for each data point(sample). Class labels are represented by numbers 1 to 4 for wrist flexion, wrist extension, hand close, hand open movements, respectively. Green stars and red stars represent true and wrong classified samples by the classifier, respectively. B) Entropy after each decision of the classifier. C) Classification accuracy calculations shown by black stars for every 200 samples.

Classification results where adaptation is applied are shown in graphs D & E. D) Entropy after each classification (adaptation is applied during classification). E) Classification accuracy calculations for every 200 samples shown by black stars. The samples where the adaptation applied marked by blue vertical triangles.
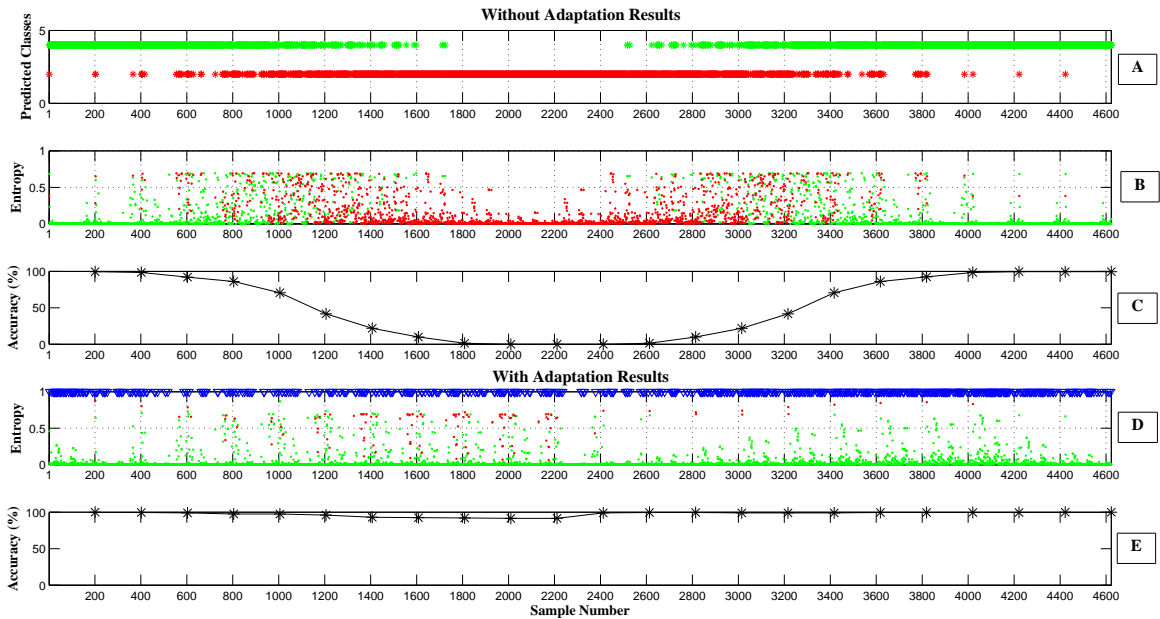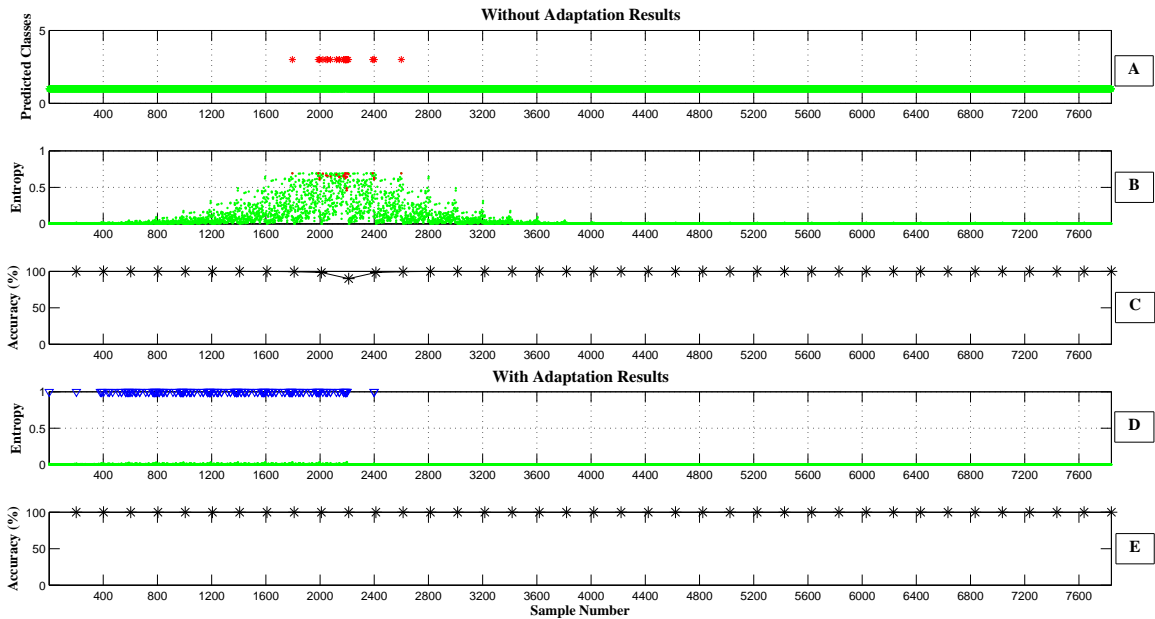
41

Figure 2.16: The classification accuracy results for type 2 distorted (DT2) for hand close movement. The classification results where no adaptation is applied are shown in graphs A, B and C. A) The output class labels of the network for each data point(sample). Class labels are represented by numbers 1 to 4 for wrist flexion, wrist extension, hand close, hand open movements, respectively. Green stars and red stars represent true and wrong classified samples by the classifier, respectively. B) Entropy after each decision of the classifier. C) Classification accuracy calculations shown by black stars for every 200 samples.

Classification results where adaptation is applied are shown in graphs D & E. D) Entropy after each classification(adaptation is applied during classification). E) Classification accuracy calculations for every 200 samples shown by black stars. The samples where the adaptation applied marked by blue vertical triangles.
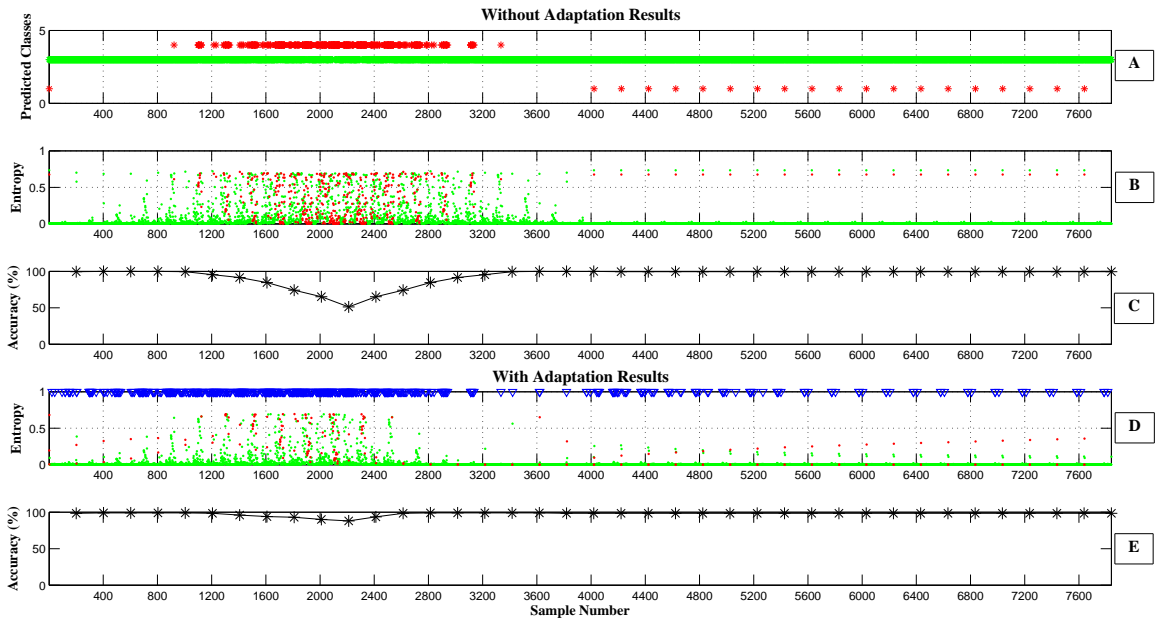
Figure 2.17: The classification accuracy results for type 2 distorted (DT2) for wrist extension movement. The classification results where no adaptation is applied are shown in graphs A, B and C. A) The output class labels of the network for each data point(sample). Class labels are represented by numbers 1 to 4 for wrist flexion, wrist extension, hand close, hand open movements, respectively. Green stars and red stars represent true and wrong classified samples by the classifier, respectively. B) Entropy after each decision of the classifier. C) Classification accuracy calculations shown by black stars for every 200 samples. Classification results where adaptation is applied are shown in graphs D & E. D) Entropy after each classification (adaptation is applied during classification). E) Classification accuracy calculations for every 200 samples shown by black stars. The samples where the adaptation applied marked by blue vertical triangles.

43

Figure 2.18: The classification accuracy results for type 2 distorted (DT2) for hand open movement. The classification results where no adaptation is applied are shown in graphs A, B and C. A) The output class labels of the network for each data point(sample). Class labels are represented by numbers 1 to 4 for wrist flexion, wrist extension, hand close, hand open movements, respectively. Green stars and red stars represent true and wrong classified samples by the classifier, respectively. B) Entropy after each decision of the classifier. C) Classification accuracy calculations shown by black stars for every 200 samples.
Classification results where adaptation is applied are shown in graphs D & E. D) Entropy after each classification(adaptation is applied during classification). E) Classification accuracy calculations for every 200 samples shown by black stars. The samples where the adaptation applied marked by blue vertical triangles.
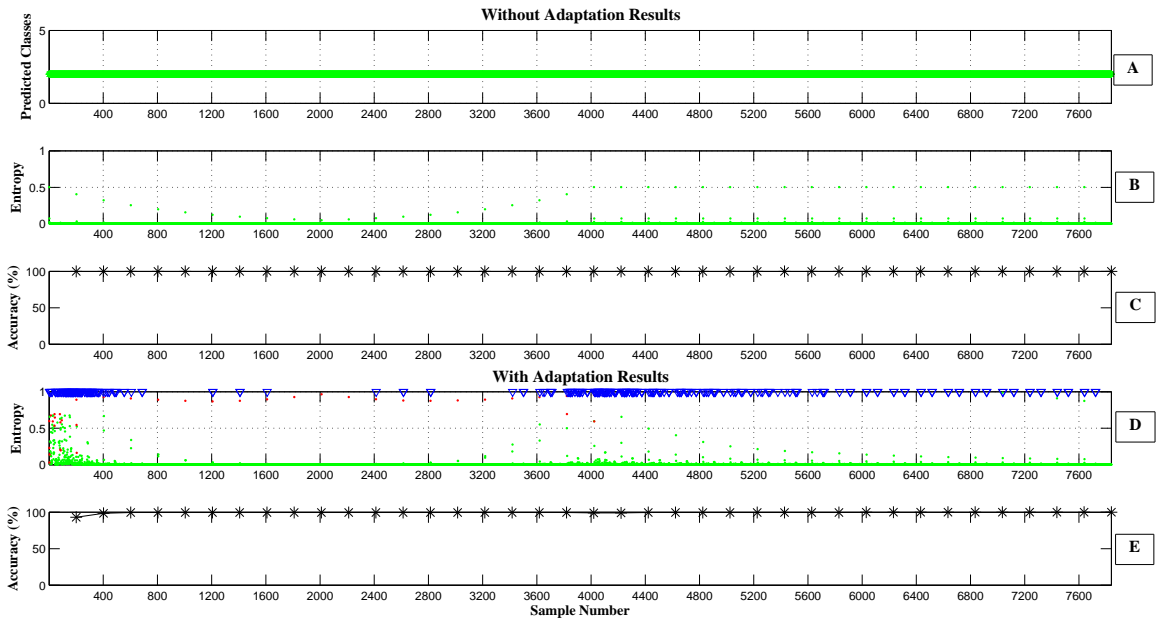
Figure 2.19: The classification accuracy results for type 3 distorted (DT3) for wrist flexion movement. The classification results where no adaptation is applied are shown in graphs A, B and C. A) The output class labels of the network for each data point(sample). Class labels are represented by numbers 1 to 4 for wrist flexion, wrist extension, hand close, hand open movements, respectively. Green stars and red stars represent true and wrong classified samples by the classifier, respectively. B) Entropy after each decision of the classifier. C) Classification accuracy calculations shown by black stars for every 200 samples.
Classification results where adaptation is applied are shown in graphs D & E. D) Entropy after each classification (adaptation is applied during classification). E) Classification accuracy calculations for every 200 samples shown by black stars. The samples where the adaptation applied marked by blue vertical triangles.
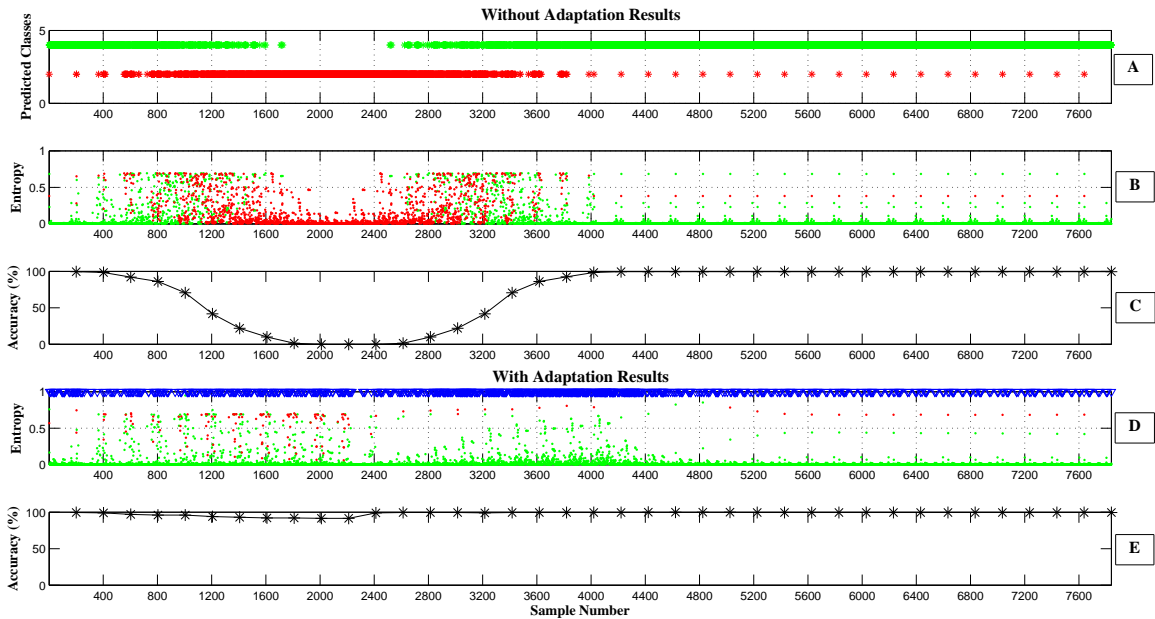
Figure 2.20: The classification accuracy results for type 3 distorted (DT3) for hand close movement. The classification results where no adaptation is applied are shown in graphs A, B and C. A) The output class labels of the network for each data point(sample). Class labels are represented by numbers 1 to 4 for wrist flexion, wrist extension, hand close, hand open movements, respectively. Green stars and red stars represent true and wrong classified samples by the classifier, respectively. B) Entropy after each decision of the classifier. C) Classification accuracy calculations shown by black stars for every 200 samples.

Classification results where adaptation is applied are shown in graphs D & E. D) Entropy after each classification (adaptation is applied during classification). E) Classification accuracy calculations for every 200 samples shown by black stars. The samples where the adaptation applied marked by blue vertical triangles.
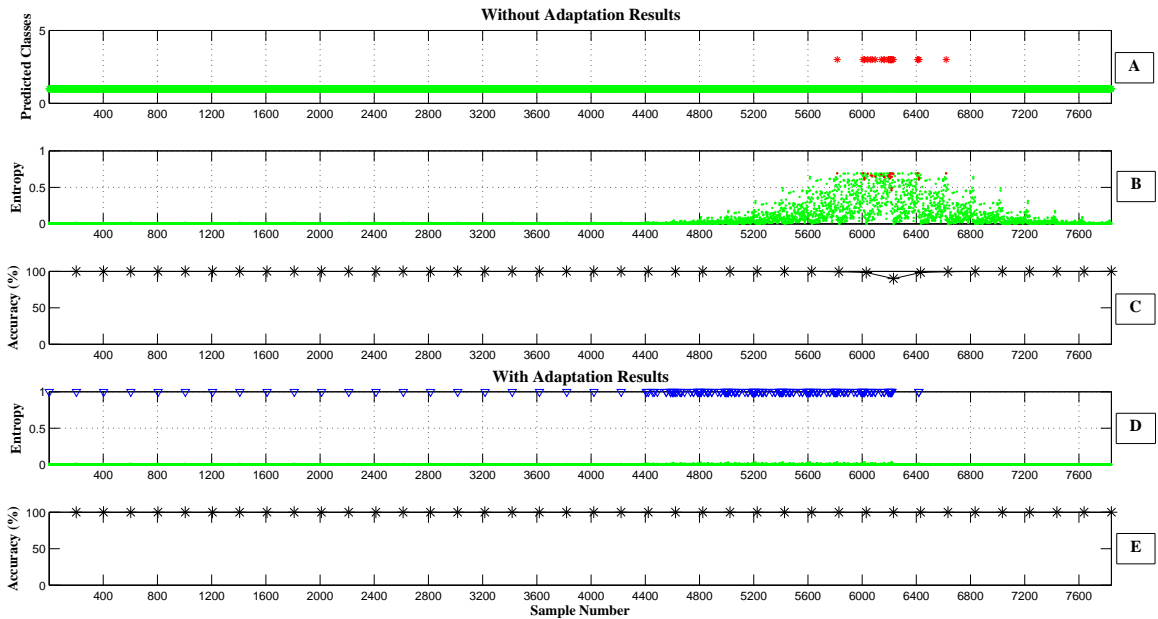
Figure 2.21: The classification accuracy results for type 3 distorted (DT3) for wrist extension movement. The classification results where no adaptation is applied are shown in graphs A, B and C. A) The output class labels of the network for each data point(sample). Class labels are represented by numbers 1 to 4 for wrist flexion, wrist extension, hand close, hand open movements, respectively. Green stars and red stars represent true and wrong classified samples by the classifier, respectively. B) Entropy after each decision of the classifier. C) Classification accuracy calculations shown by black stars for every 200 samples. Classification results where adaptation is applied are shown in graphs D & E. D) Entropy after each classification (adaptation is applied during classification). E) Classification accuracy calculations for every 200 samples shown by black stars. The samples where the adaptation applied marked by blue vertical triangles.
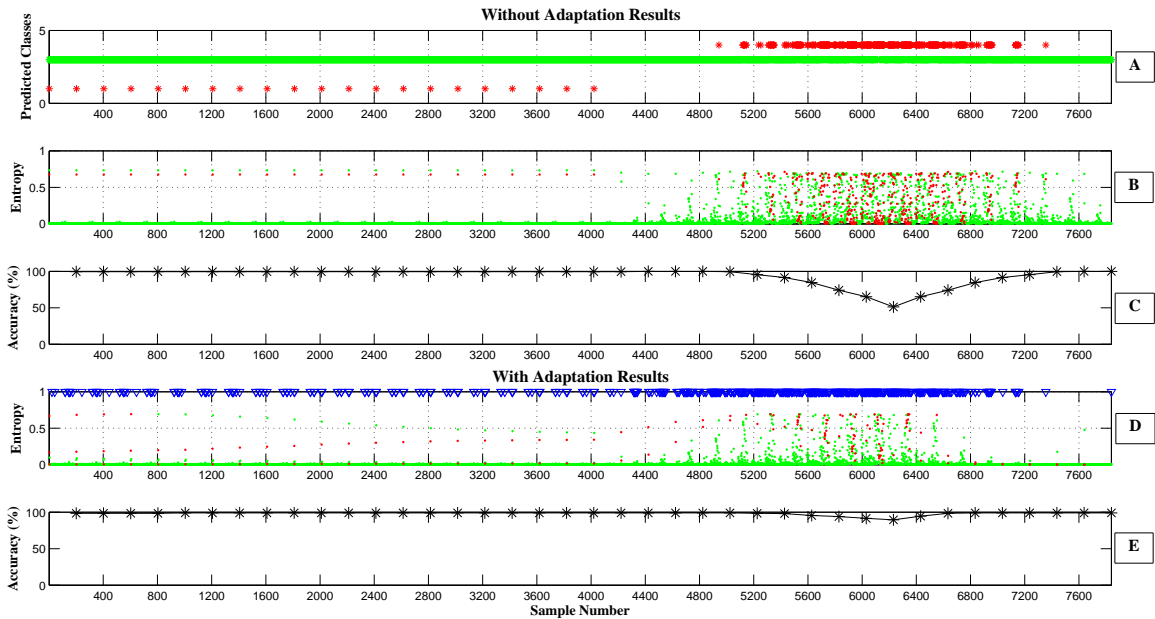
Figure 2.22: The classification accuracy results for type 3 distorted (DT3) for hand open movement. The classification results where no adaptation is applied are shown in graphs A, B and C. A) The output class labels of the network for each data point(sample). Class labels are represented by numbers 1 to 4 for wrist flexion, wrist extension, hand close, hand open movements, respectively. Green stars and red stars represent true and wrong classified samples by the classifier, respectively. B) Entropy after each decision of the classifier. C) Classification accuracy calculations shown by black stars for every 200 samples.

Classification results where adaptation is applied are shown in graphs D & E. D) Entropy after each classification (adaptation is applied during classification). E) Classification accuracy calculations for every 200 samples shown by black stars. The samples where the adaptation applied marked by blue vertical triangles.
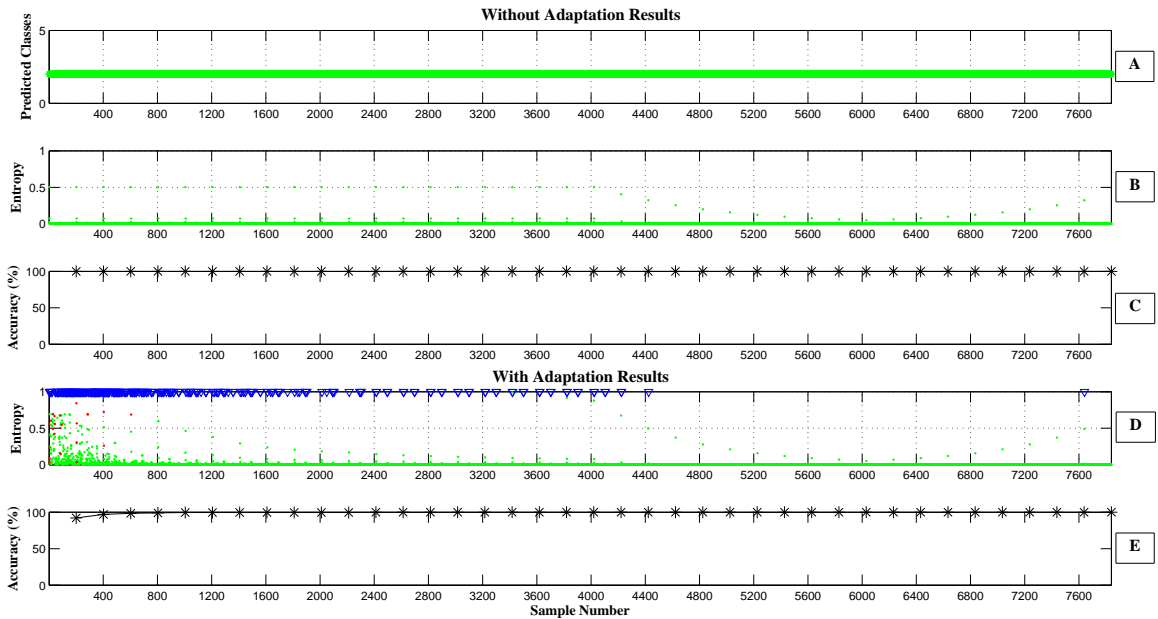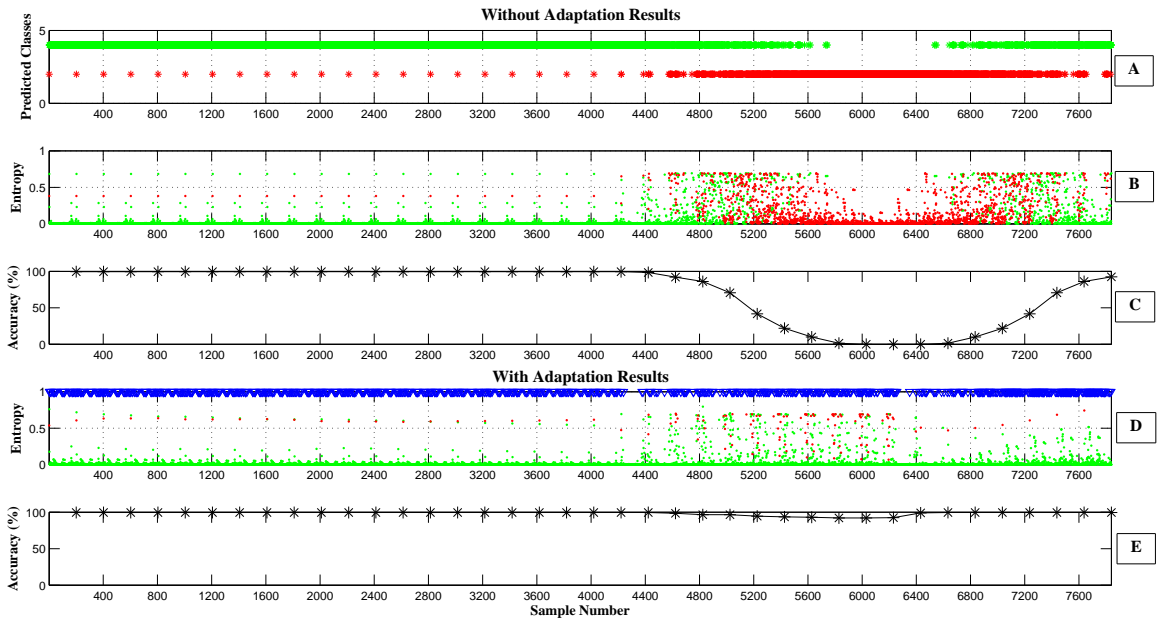
Chapter 3

NEURAL NETWORK-BASED ADAPTIVE sEMG SIGNAL CLASSIFICATION

3.1 Introduction

Two types of adaptation have been reported in the literature: user and algorithm based adaptation. Studies that have been based on the user adaptation mostly concentrate on the user training strategies to improve the user prosthetic control skills. They mostly depend on the adaptation abilities of the users to the prosthetic system. In these types of adaptation schemes, the user learns the classifier dynamics and performs movements or muscle contractions that can be distinguishable by the classifier [70]; consequently, performance improvements are observed. In the literature, the adaptation of the user to the system has been investigated. For instance, He et al. reported error rates over 11 consecutive days during prosthetic use [12]. After 3 days, a decrease has been observed in the error rates. Study demonstrates the learning/adaptation ability of the user with decrease error rates over days.

It can be said that user adaptation impacts on the system performance are observed inevitably in terms of performance improvements. However, self recovery mechanisms still required to ensure high classifier performance over time. Pattern recognition (PR) algorithms offer great performances, high accuracies have been reported in the literature [24],[18]. However, conventional pattern recognition algorithms have troubles in adaptation to the changes on the signal patterns over time. Especially for the supervised classifiers, they use parameters that are calculated at the initial training phase and classification accuracy of the classifier depends on these parameters. High classification accuracy that obtained at the beginning of the classification trials cannot be sustained due to changes on the signal patterns and the fixed parameters of the classifiers [12], [71]. Long training sessions are required to have better generalization ability of the classifier. Nevertheless, it is almost impossible to include all the possible conditions to the training data.

This problem is also valid for the neural network classifiers. The weights of the networks are the parameters of the neural network classifier. Well established weights enable to classify unseen test samples (samples that are different from the samples which are used in the training session). Conventionally, weights of the network are calculated at the end of a training session and does not modify during classification sessions. However, performance degradations may be occurred in terms of classification rates over time due to the changes in the recorded signal patterns.

Adaptive classifiers have been developed to solve this performance degradation problem. These classifiers are capable to accommodate unpredictable variations in the EMG signals. They can simply improve the classifier performance and reduce the user effort during prosthetic use. When system performance starts to deteriorate, parameters of the classifier updated. This approach aids to track changes in the feature space and significantly recovers the performance degradations. Training strategies have been developed to update classifier parameters that can be used during classifications. Therefore, robust and reliable unsupervised approaches are on demand.

In the present study, we aimed to develop an unsupervised adaptation technique that is capable to detect adaptation required cases without any need for supervision by the user or someone else. Also an entropy history buffer property is included to the technique to avoid overtraining and improve the robustness of the adaptive classifier.

In this chapter, the details about the data acquisition settings are given first. Afterwards, the developed adaptive neural network classifier is introduced. Classifier, neural network and the other system components that constitute the adaptive algorithm are explained in different sections. The classification results for experimental sEMG data from 2 subjects are presented. The results are discussed and main contributions of the developed classifier are presented at the end of the chapter.

3.2 Methods

3.2.1 Data Acquisition

3.2.1.1 Experimental setup

Data acquisition experimental setup consists of Myo armband, a Bluetooth adapter and PC(Intel Core i5, 3.20GHz CPU, x64 bit windows 8 pro opearating system and 4GB RAM).

Myo armband is a wearable gesture control device released by Thalmic Labs Inc. in 2001. It has eight surface EMG electrode pairs and inertial measurement unit (IMU) containing gyroscope, accelerometer and a magnetometer. Only the EMG data stream is used in the study. The sampling rate of the device is 200 Hz. The device sends the digitized EMG signals to the PC using Bluetooth technology.

There are several advantages of using Myo armband in data acquisition experiments. It is like a bracelet which has elastic material and can easily be worn to the forearm. On the other hand, combination of the design of the electrode and stainless steel dry electrodes that is located on the device provides good skin electrode contact and enables recording high quality and reliable signals. When it is fit to the arm of the user properly, no further preparation required before using the device. Since several preparation steps (removing hair, cleaning skin etc.) are need to start recording for the conventional data acquisition configurations, this device superior to other conventional methods due to this property. Consequently, Myo armband eases collecting EMG data from forearm while performing movement tasks.

3.2.1.2 User interface

A MATLAB interface was implemented to manage subject, experimenter and the device interactions during data acquisition processes. Experimenter guided the subject about the execution time intervals of the forearm movements by tracking the command flow in the user interface. MATLAB packages (developed by Mark Tomaszewski), which provides the control of EMG and the software interactions to collect EMG data recordings from the EMG electrodes, and Thalmic labs released software development kit (SDK) files of the Myo armband are utilized during the implementation of the interface. The graphical user interface simply displays the name of the movements that are required to initiate instantly. Movement execution time displayed with a countdown and also for the rest states between the movements. In resting state a cue shown to inform the user for the next movement. The commands that show the movement names in the movement set are periodically displayed in the interface until intended experiment time is achieved.

3.2.1.3   Experimental environment

Myo armband was on the same location on the arm of the subject during a data recording session. Subject was on a comfortable chair in a neutral sitting posture. The posture of the body, the angles of the joints, the location and the direction of the arm were approximately same during the experiments. Elbow angle (between forearm and the upper arm) was 90 degree and it was 0 degree between upper arm and the body of the subject approximately. Forearm was positioned on a soft rounded pad (object) touching the forearm at the wrist, considering same direction of the palm for each experiment. Rest of the forearm was not reclined to anywhere, only upper arm has support from the back side of the chair. So, no pressure applied onto Myo armband while performing movements. Pressure on armband may change the electrode locations and the amount of area that the electrode contacts the skin. In this case, it is not possible to ensure same electrode configurations due to possible electrode shifts. It can be resulted in fluctuations on the acquired signals. Possible pressure to the Myo armband while it is on the arm may lead significant impedance change on the skin-electrode interface, so we avoided such disturbances on the position of the Myo armband and the pressure on its electrodes.

3.2.2   Data Acquisition Sessions

Performing the movement set once a time will be called "trial" and multiple repetition of movement set for a specified time interval will be called a "session" of data acquisition experiments in this and the following sections.

3.2.2.1   Subjects

Two able-bodied subjects are participated in data acquisition sessions of the study. SEMG signals were obtained from 2 female subjects to be used in the following classification experiments. Subjects had no known neurological and

physiological muscle related disorders.

3.2.2.2 Movement set

Five different movements are performed in predetermined order for each trial. Each subject is informed by the experimenter about motion beginning and end times by using the developed interface during data acquisition sessions. Between-movement transition parts are removed from the acquired raw signals to obtain clear and distinct data patterns for each class corresponding to movement types. Movements that are executed by subjects was in the order: hand close (HC) (full grasp), hand open(HO), hand grasp(HG)(half grasp), wrist flexion(WF), wrist extension(WE) respectively as illustrated in Figure 3.1.

Hand Close	Hand Open	Hand Grasp	Wrist Flexion	Wrist Extension
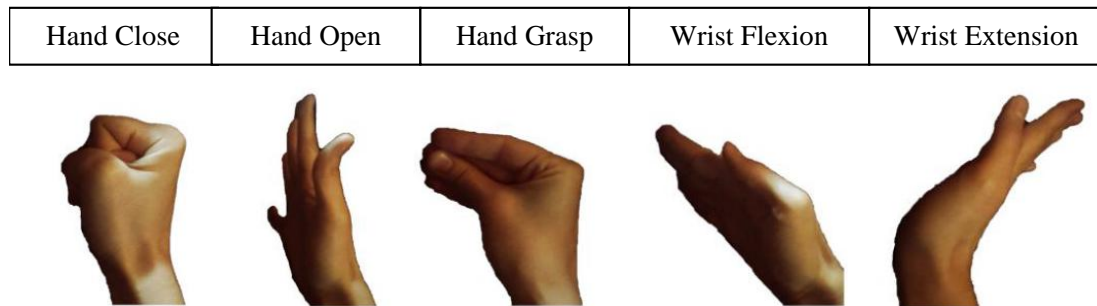
Figure 3.1: The movement set.

3.2.2.3 The details of the sessions

Before starting a session, armband is placed on the dominant forearm of the participant to the thickest muscle bundle; approximately 5 cm below elbow corresponds to a region where superficial flexor and extensor muscles locate underneath. Each movement contractions are held 5-6 seconds and time interval between the movements is 10 seconds to prevent muscle from fatigue and unintended contractions (e.g. twitches). Muscles are in rest in resting state intervals. Subject specific voluntary contractions are executed. So, there is no restricted level of force need to be applied to perform the movements. Trials are repeated

54

30 times for each subject and there is 15 seconds between the trials. Two sessions are conducted for each participant. Total time to conduct a session for a subject is taken at around 50 minutes. One of the data acquisition session is illustrated in Figure 3.2.
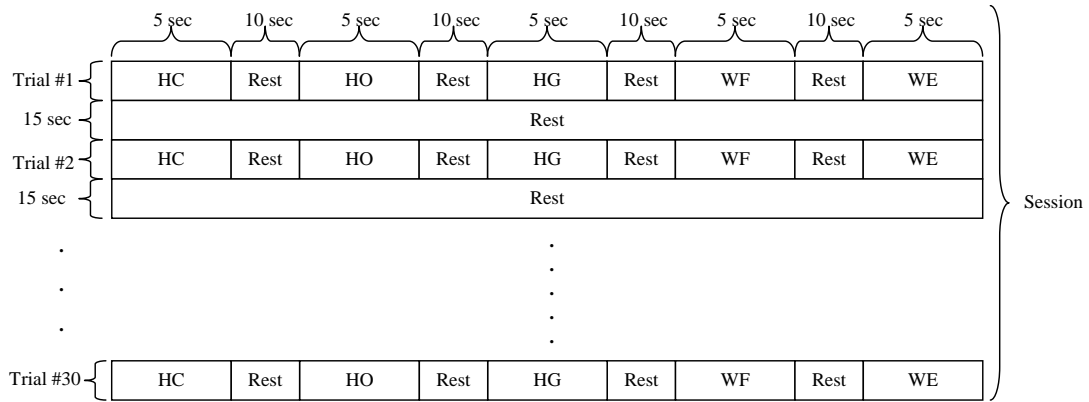
Figure 3.2: The data acquisition session.

3.2.3 Adaptive Classifier

The algorithm of the developed adaptive classifier based on a neural network is shown in Figure 3.3.

sEMG signals are separated into the time windows and the features are extracted from each window. The features are the sEMG signal samples that will be fed to the network. When a new sEMG data sample is arrived to the network, network process the sample and outputs the probability calculations for each class. The entropy is calculated utilizing the network outputs. The entropy values are stored in a buffer; last calculated entropy value is located at the end of the buffer. The buffer size determines the memory size of the system for the latest classification. The buffer is called "entropy history buffer" in this study. The entropy history buffer is checked after every network output. If the entropy history buffer is not full, current sample are directly classified according to the neural probability outputs. Otherwise, if the buffer size is full, all entropy values in the buffer are checked whether they fall into the predetermined entropy

55

threshold interval or not. If all the entropy values are under the predetermined threshold, adaptation process is applied. The network weights are updated with the last sample by utilizing back propagation algorithm. On the other hand, if one or more entropy value exceeds the entropy threshold in the full sized buffer, the entropy history buffer is cleared and the entropy values are started to store for the next samples. When the sample classification process is completed, prosthetic may take action according to the classifier decision. The "motion" step is not conducted in this study, it is included to the figure only to show next possible step in real time prosthetic use.
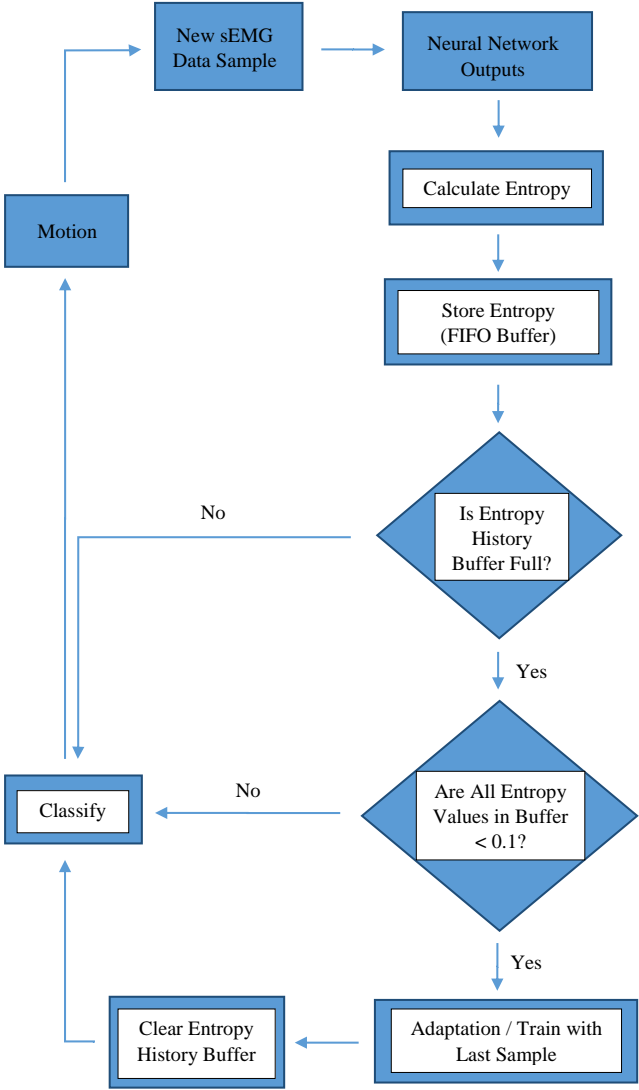
Figure 3.3: Flowchart of the adaptive neural network algorithm.

3.2.3.1 The classifier: neural network

A three-layer feed-forward neural network is used as a classifier in this study. Network inputs are features (root mean square (RMS) and wavelength (WL)) that are extracted from moving 200ms length and 150ms overlapping time windows. Time window length is an important parameter for the classification decisions. It should not be too long to prevent the system from late decisions. On the other hand, it should not be too short to avoid misrepresentation of the signal patterns. In this sense, the optimal window length is determined according to previous studies [72].

Feature selection is done empirically comparing the classifier performance among time domain features. As it is indicated in the study, comparison among classification results have revealed wavelength (WL) feature superiority to other time domain features such as Willison amplitude, mean absolute value, variance etc. [14].

The data provided from all 8 channels of the Myo armband is processed in this study. Two features from each channel correspond to 16 input neurons for the network. Sigmoid functions are used at the 6 hidden neurons as activation function. Softmax function is used at the output layer which consists of 5 neurons. Trade off between complexity and the classification accuracy is considered to determine optimal network structure. Learning rate is the other parameter of the network and determined empirically too. The network structure is illustrated in Figure 3.4.

Softmax function returns output values which are the posterior probabilities of each target class. All the output values fall in a range between 0 and 1 and the sum of them equals 1. It is the main advantage of the softmax function and helps to make decisions. The output neuron which has the highest value also has the highest probability of belonging to a particular target class.
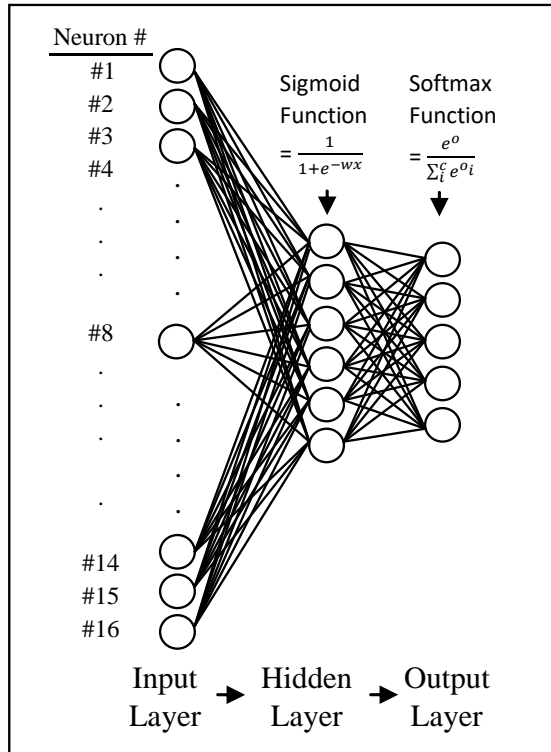
Figure 3.4: The structure of the neural network.

Back propagation algorithm is the training algorithm of the network. It is used in the initial training phase to calculate the network weights. After completing the training phase, test data classification experiments are conducted. During the classification phase, back propagation is also enabled to update network weights if the adaptation required conditions are met. Since the target label are not known during test data classifications, the network is utilized from its own class decisions to set target label during the network weights updates. In other words, labeled samples by the classifier are used to retrain the network and weights are updated accordingly. Thus, an unsupervised adaptation process is applied.

3.2.3.2 Adaptation using "entropy"

In the unsupervised adaptation schemes, important issues such as when to adapt and how to adapt should be considered as it is mentioned in [31] to obtain a

reliable and efficient way of adaptation. In order to develop a reliable adaptive scheme, adaptive classifier dynamics are constructed with these parameters taken into consideration:

- **the frequency** of the adaptation,

- **a confidence metric** to prevent the unsupervised classifier from adapting according to the previous unreliable classification results,

- **adaptation size** to prevent the unsupervised classifier from overfitting

- **disturbing the convergence properties of the classifier**.

Entropy is our confidence metric that controls the network outputs and decides when to update the network weights. High entropy means low confidence for the particular classifier decision. Conversely, low entropy means high confidence. Since the cases in which adaptation is required is detected by the entropy threshold, this threshold should be well defined to prevent the system from the degradations in the classification accuracy. Low entropy threshold may lead to no improvement in the classification accuracy (only adaptation will be in the most confident interval, this may not make any change in the overall classification accuracy) and too high entropy threshold may increase the risk of come across non reliable classifier output (may cause updating the network weights using wrong labeled samples). Therefore, entropy threshold is determined to 0.1 after several empirical evaluations. The entropy also determines the frequency of the adaptation. There is neither periodical nor incremental adaptation. The algorithm detects the time points which an adaptation is required.

Since there is no batch learning applied during the network updates in our design, adaptation size becomes a more important parameter in the algorithm. Learning rate is a critical parameter to adjust adaptation size of the unsupervised neural network classifier. Network updates its weights using only the latest network inputs by online back propagation update rule and the learning rate is used for this rule. Therefore, an optimal value is determined for learning rate

which is not too big to update the weights to the same class instantly; such a fast adaptation to a single class can lead to decrease in the overall classification accuracy of the neural network. On the other hand, learning rate was not too small so that insignificant improvements on the adaptation performance may be avoided.

Entropy is calculated after each output of the network and changes in the entropy values are tracked by the adaptation algorithm. If the entropy of the output of the classifier is smaller than a predetermined threshold (0.1), adaptation process is applied since the result of the classification is assumed to be reliable. The entropy of a classification output for a network input is expressed as:

$$E(t) = -\sum_{c=1}^{C} netOut_c(t) \; ln(netOut_c(t)) \tag{3.1}$$

where C is total number of classes, $netOut$ is the output of each output neuron of the network which corresponds to the posterior probabilities of the sample t, to belong to a class.

An entropy history buffer is added to the adaptation algorithm to improve performance and robustness of the system. In the classification phase, after each entropy calculation using Equation 3.1, entropy values are stored in a buffer which is called "entropy history buffer" . When the capacity of the buffer is full, entropy value of next upcoming input is calculated again using Equation 3.1 and if it is below a threshold (0.1), adaptation process is applied. The size of the "entropy history buffer" is empirically determined as 10. After every adaptation process the buffer is cleared and started to stored again the entropies of the upcoming classifications.

3.3 Results

Training and test data sets are constructed from the collected raw EMG signals for each session of the each subject. The signals are divided into time windows and the features are extracted from each sliding time window. The resultant

samples are labeled for each class to obtain separate movement patterns. First trial's data in a session are used as training data, the rest (29 of them) are used as test data. Training and test phases of each session are conducted separately. The construction of the test and training data sets from a session data is shown in Figure 3.5.

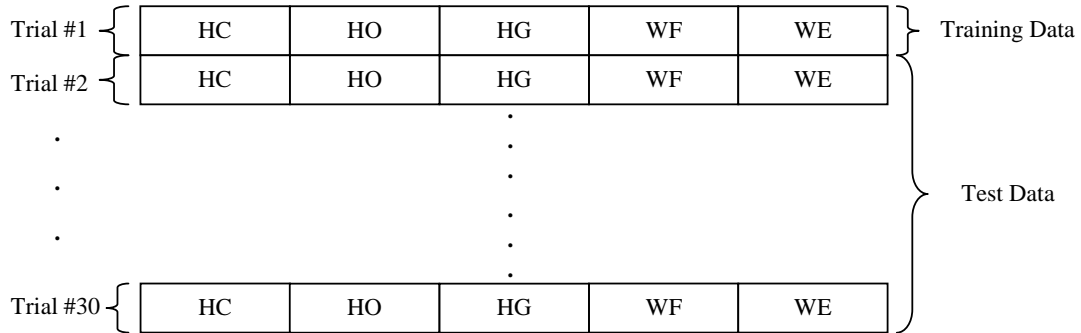| Trial #1	HC	HO	HG	WF	WE	Training Data
Trial #2	HC	HO	HG	WF	WE	
.		.				
.		.				Test Data
.		.				
Trial #30	HC	HO	HG	WF	WE	

Figure 3.5: The construction of training and test data set from a session.

The network weights are randomly initialized in an interval between 0.01 and -0.01 as it is recommended in [73] (cited from book [73]: "initial value of weights large in magnitude, weights sum may also be large and may saturate the sigmoid, so initial weights should be chosen close to zero") for the initial training phase. The learning rate is determined as 0.05 to be used for all the training and test phases. The stopping criteria of the training phase was reaching 100% classification accuracy in the training (0 classification error) and obtaining an average entropy over classification outputs of an epoch which is smaller than 0.01. The classification accuracy and the average entropy is calculated at the end of every epoch by feeding all the training data samples into the network again and classifying with last updated weights.

At end of the network training, the calculated weights are stored to be used in the test phases. The training phase is repeated 10 times with randomly initiated weights. Consequently, 10 different weights are obtained at the end of conducted training phases for each session data of each subject. All the parameters are same (e.g. learning rate, entropy history buffer size and entropy threshold) for all the

61

experiments. Classification phases are conducted 10 times with the previously trained and calculated 10 weights for each session data of the each subject. Classifier performance is reported by averaging the recognition accuracies of all (10) test phases of each session. The classification accuracy is a widely used metric to evaluate classification performance of the classifiers and it is calculated as:

$$ClassificationAccuracy = \frac{\text{Number of Correctly Classified Samples}}{\text{Number of All Classified Samples}}$$

3.3.1 Entropy History Buffer Size Comparison

In order to demonstrate effect of entropy history buffer size on adaptation performance, classification results are compared when entropy history buffer size equals 1 ($EHB1$) and equals 10 ($EHB10$). Same initial weights are used for both experiments. The mean accuracy results of the experiments are presented in Table 3.1 for $EHB1$ (on the left) and for $EHB10$ (on the right) respectively. The mean accuracy results are reported for three different conditions:

- **Condition 1**, in the case of when no adaptation is applied. We call them "WoA condition".

- **Condition 2**, in which adaptation is applied and the weights are updated using the algorithm shown in Figure 3.3. We call them "WA condition".

- **Condition 3**, in which the weights are updated using the algorithm shown in Figure 3.3 but reset to the value at the beginning of each movement type. In other words, the adaptation is applied during a movement type is executed but realization of the adaptation is discarded before starting the execution of the next movement type. We applied this test case to show whether the adaptation algorithm improves the classification accuracy during executing any movement type. We call this condition "$WAin$ condition".

In Table 3.1, the accuracy results are presented for 29 consecutive trials for each three different conditions (WoA, WA, WAin) (In this table, trial numbers represent each trial classification accuracy results which are calculated using Equation 3.3). WA and WoA accuracy results are compared. Improvements in the WA results are highlighted with bold fonts and decreased examples are represented with bold and underlined fonts. $EHB10$ is superior to $EHB1$ according to these results. Because, when the results for condition WoA and WA are compared, decreases in the classification accuracy is more than the improvements. For instance, an improvement of 2% is observed in the accuracy of trial 13 of the $EHB1$ experiment but a decrease is observed in the next trial (trial 14) with 1% in the overall accuracy when the adaptation is applied (WA condition). This decrease can be explained with over fitting. On the other hand improvements are mostly observed in the $EHB10$ results and it is valid for $WAin$ condition too; WA values are higher than $WAin$ values in most of the trials. On the other hand, in comparison with $EHB1$ results more improvements are observed when the entropy history buffer size is 10 (EHB10). These results indicate the requirement of entropy history approach. Therefore, using entropy history buffer in the algorithm provides controllability when applying the adaptation and enables to avoid applying unreliable unsupervised adaptations.

| Entropy History Size=1 | | | | Entropy History Size=10 | | | |
| Classification Accuracy (%) | | | | Classification Accuracy (%) | | | |
Trial Number	WoA	WAin	WA	Trial Number	WoA	WAin	WA
1	96.35	96.08	96.5	1	96.35	96.35	**96.38**
2	98.8	98.73	98.88	2	98.8	98.77	98.76
3	95.09	94.0	**94.52**	3	95.09	95.04	95.05
4	95.07	94.96	95.16	4	95.07	95.05	**95.08**
5	95.95	95.7	96.18	5	95.95	95.84	95.95
6	91.25	89.87	**90.77**	6	91.25	91.37	**91.42**
7	92.27	90.5	**90.88**	7	92.27	92.27	**92.31**
8	92.31	92.41	93.26	8	92.31	92.45	**92.49**
9	93.98	94.5	94.91	9	93.98	94.07	**94.14**
10	93.04	94.47	94.99	10	93.04	93.36	**93.51**
11	94.44	95.29	96.72	11	94.44	94.66	**94.69**
12	90.19	91.27	92.91	12	90.19	90.61	**90.65**
13	91.93	92.87	93.28	13	91.93	92.29	**92.35**
14	97.22	96.28	**96.33**	14	97.22	97.35	**97.35**
15	95.59	94.06	**94.54**	15	95.59	95.6	**95.64**
16	94.98	93.77	**94.16**	16	94.98	95.0	**95.1**
17	95.49	94.72	**95.24**	17	95.49	95.91	**96.01**
18	94.73	94.59	94.91	18	94.73	95.39	**95.52**
19	93.05	93.42	93.83	19	93.05	94.3	**94.36**
20	94.58	95.36	95.72	20	94.58	95.38	**95.45**
21	96.44	95.56	**95.81**	21	96.44	96.78	**96.79**
22	93.81	94.04	94.44	22	93.81	94.39	**94.51**
23	90.47	91.45	91.84	23	90.47	91.86	**91.88**
24	94.67	95.75	96.14	24	94.67	95.74	**95.79**
25	94.38	94.5	94.88	25	94.38	95.64	**95.67**
26	94.98	93.37	**93.66**	26	94.98	95.06	**95.09**
27	94.52	93.91	94.54	27	94.52	94.95	**95.0**
28	93.81	91.84	**92.21**	28	93.81	94.42	**94.45**
29	90.65	88.74	**89.91**	29	90.65	91.43	**91.53**
Mean	94.14	93.86	94.38	Mean	94.14	94.53	**94.58**

Table 3.1: The overall mean accuracy (%) results when entropy history buffer size equals 1 and 10 respectively.

3.3.2 Subject Specific Results

The average of the two sessions' overall classification accuracies are calculated for each subject (two sessions are conducted for each subject). Overall mean accuracy results are reported as bar graphs for the Subject 1 and Subject 2 respectively in Figures 3.6 and 3.7.
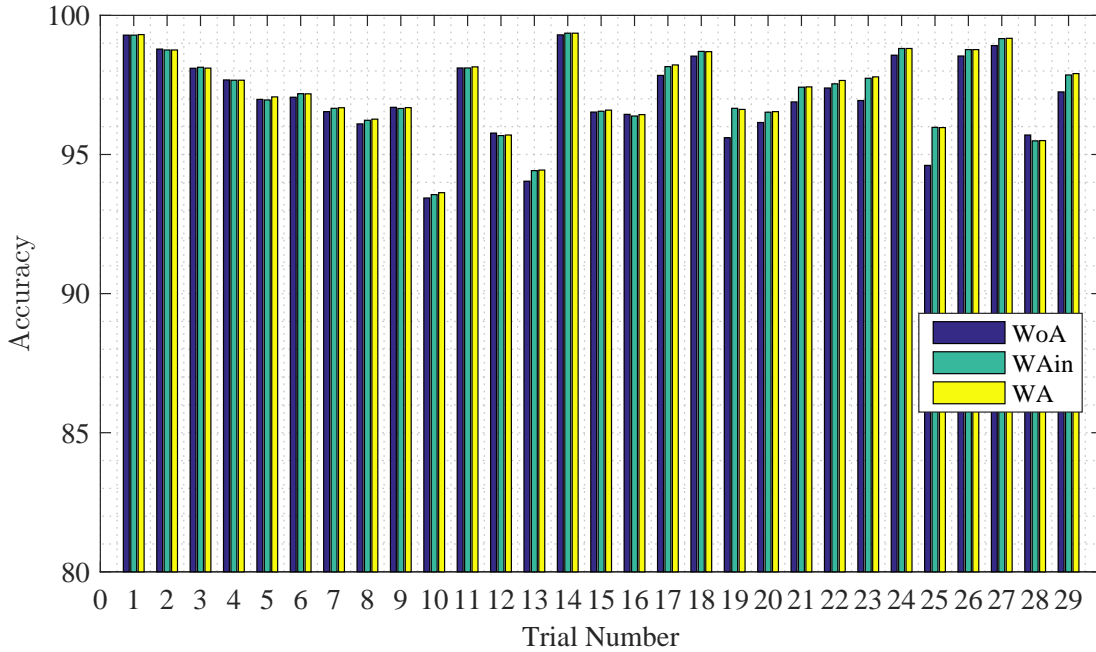

Figure 3.6: Overall classification accuracy(%) for Subject 1.

3.3.3 Class Specific Results

Class specific mean accuracy results of the subject 1 are presented in the Figures 3.8, 3.9, 3.10, 3.11, 3.12 for the movements HO, HC, HG, WF and WE respectively. The presented results are average of the classification accuracy results of two sessions that is conducted by the subject 1.
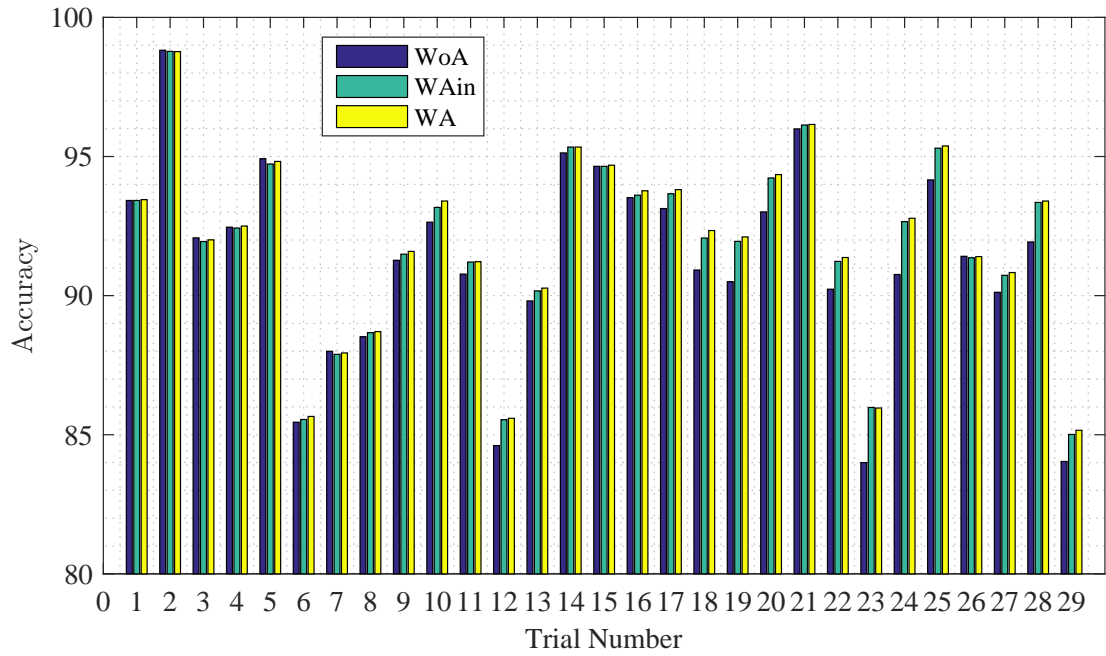
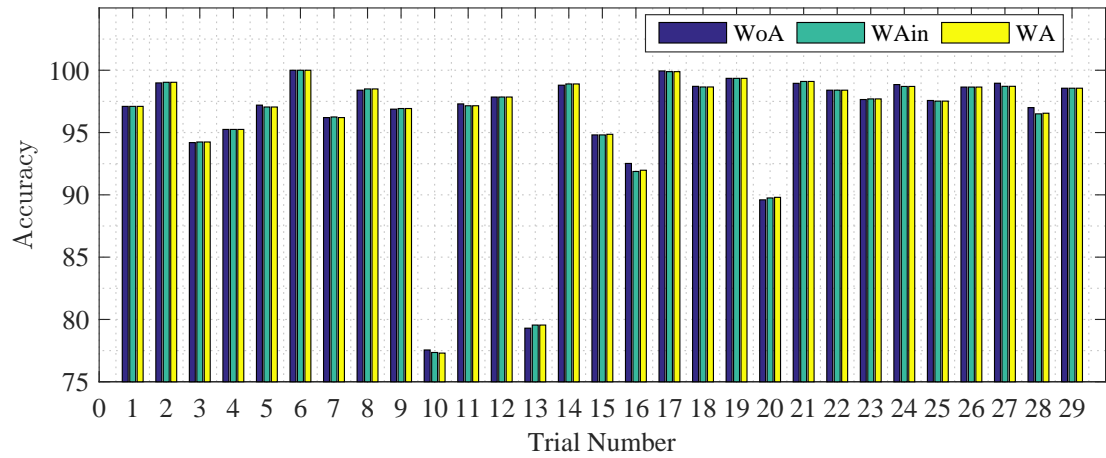Figure 3.7: Overall classification accuracy(%) for Subject 2.

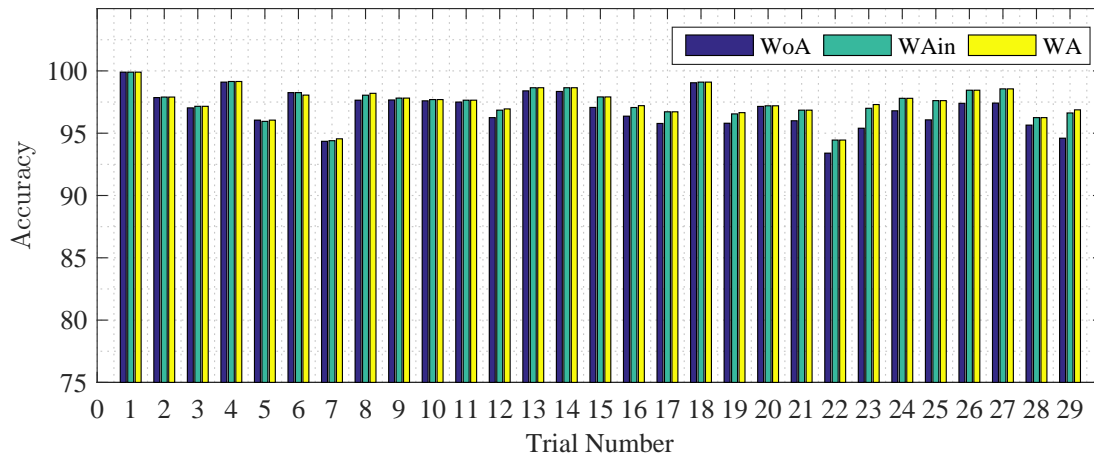Figure 3.8: Classification accuracy(%) for Subject 1 for hand open (HO) movement.

Figure 3.9: Classification accuracy (%) for Subject 1 for hand close (HC) movement.
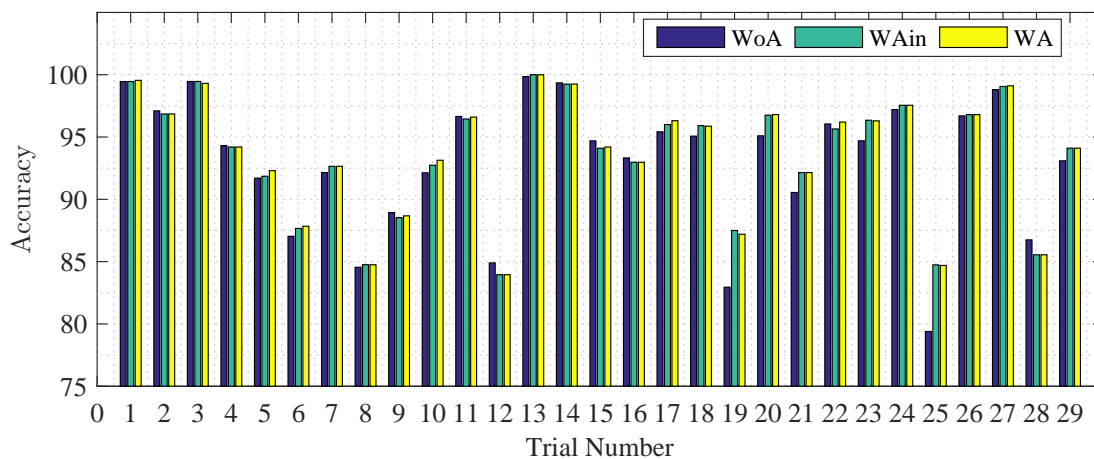

Figure 3.10: Classification accuracy (%) for Subject 1 for hand grasp (HG) movement.

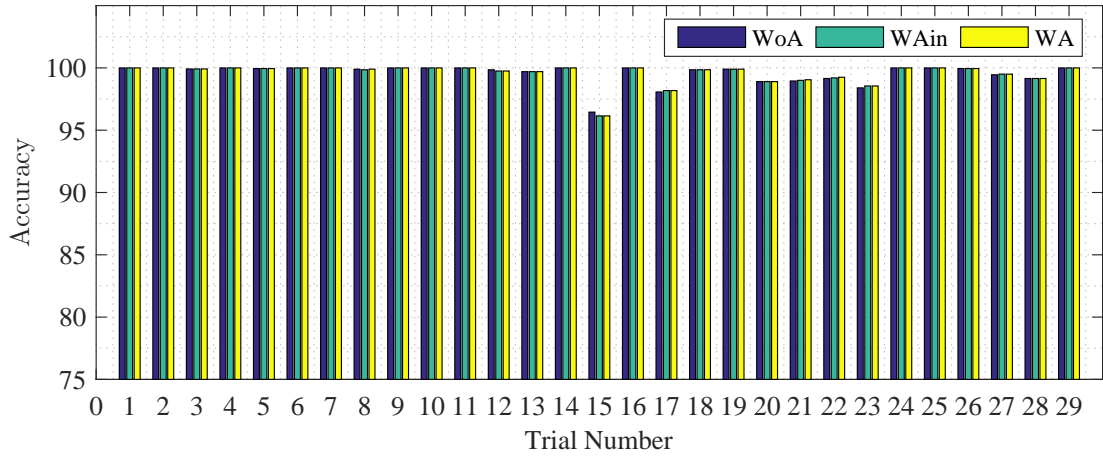Figure 3.11: Classification accuracy(%) for Subject 1 for wrist flexion (WF) movement.
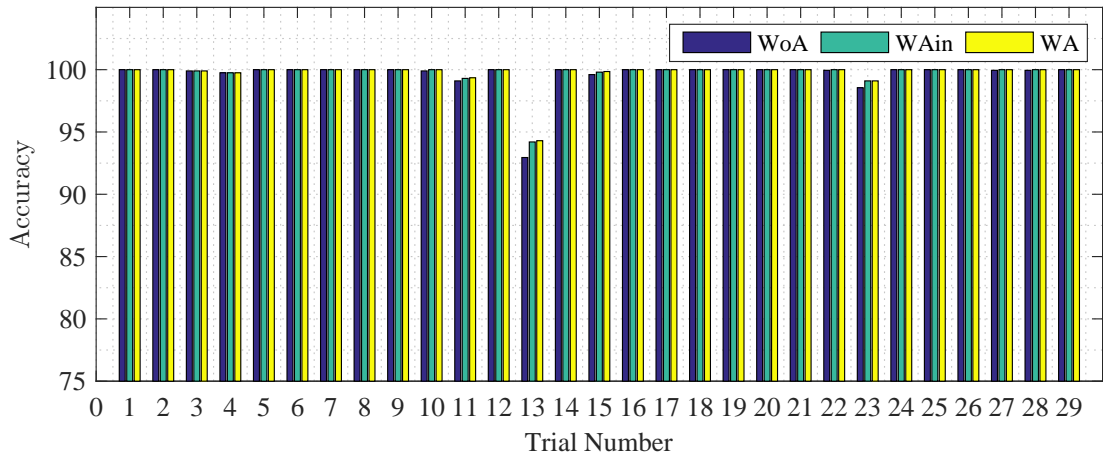

Figure 3.12: Classification accuracy(%) for Subject 1 for wrist extension (WE) movement.

3.4 Discussion

3.4.1 Entropy History Buffer Size Comparison

Entropy history buffer is inserted into the adaptation algorithm to avoid over fitting and construct a robust algorithm which is not too sensitive to transients and

sudden degradations in the signals. Especially entropy history is significantly advantageous for the cases in which many adaptation applicable (confident) samples are consecutively fed to the neural network classifier.

3.4.2 Subject Specific Results

The subject specific classification results demonstrate that our adaptation algorithm applied on a neural network classifier improves the classification performance of a non-adaptive neural network classifier. Even when lower classification accuracies than the other trials are observed in classification accuracy when no adaptation (WoA) is applied (such as 84% (WoA) in trial 23 of subject 2), notable improvement is observed when classification accuracy results are compared (WoA and WA).

3.4.3 Class Specific Results

Classification accuracy results are reported for Subject 1 for each class. No significant decrease is observed in the accuracy results, when the results for the conditions in which adaptation is applied (WA) and is not applied are compared. On the other hand, in some of the trials' classification accuracy results no significant improvements are observed when adaptation is not applied (WoA) and is applied (WA) classification accuracy results are compared. This can be explained with high WoA (when no adaptation applied) classification accuracy results. In these trials adaptation is not required to apply already.

It can be valid also for the first trial results in which the adaptation process may not significantly change the network weights. Therefore, no change in the classification accuracy occur.

Chapter 4

CONCLUSIONS

In the present thesis two-channel differential sEMG signals are simulated by utilizing a sEMG model. The simulated signals corresponded to four different movement types such as hand close, hand open, wrist extension and wrist flexion. The amplitude of simulated sEMG signals are then changed for each movement to simulate the distortion effects caused by the conditions such as loose conduct between the skin and the electrode and sweating. Distortion is created on the signals basically by gradually changing the amplitude of the signals. The amplitude change in the signals for one channel was maximum 50%. The adaptive neural-network classifier proposed in the present thesis was developed using these sEMG signal simulations. After the development phase, the classification and adaptation performance of the present classifier is studied and validated using sEMG recordings obtained from two able-bodied subjects. Our results indicate that the utilization of entropy associated with the classification decisions of the neural network as a confidence metric is appropriate for reliable adaptations. An entropy threshold is used in the system to determine whether a classification decision is confident or not. If entropy associated with a decision is below this threshold, the decision is considered confident and the network is trained using the latest input vector. In this sense, decreasing the entropy threshold in the system would improve the reliability of the adaptations. However, decreasing this threshold would also decrease the probability of realization of adaptations and consequently adaptation

capability of the system. Therefore, the designer of the prosthetic controller needs to determine the value of the entropy threshold by considering the trade-off between the reliability of the adaptations and the number of adaptations. In order to further improve the reliability of the adaptations, we additionally implemented a FIFO buffer into the system to store the entropies associated with a number of latest classifications. The adaptations in the system realized only when all entropy values in this buffer are below a certain threshold. Increasing the size of this entropy history buffer would improve the reliability of the adaptations while decreasing the probability of realizing an adaptation.

4.1   Advantages of the System

In the present system, there is no need to store the sEMG input vectors during the adaptation or classification phase. Only the latest entropy values are required to be stored into a history buffer to determine if the latest sEMG input vector is suitable to be used for online learning, which realizes the adaptation in the system. In this sense, the algorithm can track the entropy changes and detect the adaptation required conditions by using the entropy history buffer. Thus, the probability of application of adaptation is under control and the neural network is prevented from overtraining. It can be said that, the weights of the neural network are adapted to the upcoming signal inputs through adjusting by online learning gradually according to the signal dynamic changes over time. Therefore, it is not required to re-train the network during the classification phase (starting from the random initial weights and using all training data). Furthermore, the adaptation step of the present algorithm is easy to implement and computationally efficient, thus the present approach can be a promising solution to improve the performance of the prosthetic limb decoders (controllers).

4.2 Limitations of the System and Future Improvements

In the present study, the adaptation performance and classification accuracy of the developed algorithm was studied offline using sEMG signals previously recorded from able-bodied subjects performing hand gestures. Real time (online) prosthetic hand control experiments are required to be conducted to evaluate the applicability of the algorithm in clinic applications. In addition, the performance of the classifier proposed in the present thesis was studied using the sEMG signals recorded from able-bodied subjects instead of the ones recorded from amputees. Although it is reported in the previous studies that the prosthetic hand control performance of amputee and able-bodied subjects is similar to each other, the performance of the classifier presented here should also be studied with recordings from amputees.

Bibliography

[1] R. W. Wirta, D. R. Taylor, and F. R. Finley, "Pattern-recognition arm prosthesis: a historical perspective-a final report.," *Bulletin of prosthetics research*, pp. 8–35, 1978.

[2] P. Zhou, M. M. Lowery, K. B. Englehart, H. Huang, G. Li, L. Hargrove, J. P. A. Dewald, and T. A. Kuiken, "Decoding a new neural machine interface for control of artificial limbs.," *Journal of neurophysiology*, vol. 98, no. 5, pp. 2974–82, 2007.

[3] T. a. Kuiken, G. Li, B. a. Lock, R. D. Lipschutz, L. a. Miller, K. a. Stubblefield, and K. Englehart, "Targeted Muscle Reinnervation for Real-Time Myoelectric Control of Multifunction Artificial Arms," *NIH Public Access*, vol. 301, no. 6, pp. 619–628, 2009.

[4] K. Englehart, B. Hudgins, P. A. Parker, and S. Member, "A Wavelet-Based Continuous Classification Scheme for Multifunction Myoelectric Control," *IEEE Transactions on Biomedical Engineering*, vol. 48, no. 3, pp. 302–311, 2001.

[5] A. Radmand, E. Scheme, and K. Englehart, "A Characterization of the Effect of Limb Position on EMG Features to Guide the Development of Effective Prosthetic Control Schemes," in *36th Annual International Conference of the IEEE Engineering in Medicince and Biology Society*, pp. 662–667, 2014.

[6] A. J. Young, L. J. Hargrove, and T. a. Kuiken, "The effects of electrode size and orientation on the sensitivity of myoelectric pattern recognition systems

to electrode shift," *IEEE Transactions on Biomedical Engineering*, vol. 58, no. 9, pp. 2537–2544, 2011.

[7] L. Hargrove, K. Englehart, and B. Hudgins, "A training strategy to reduce classification degradation due to electrode displacements in pattern recognition based myoelectric control," *Biomedical Signal Processing and Control*, vol. 3, pp. 175–180, 2008.

[8] A. Fougner, E. Scheme, A. D. C. Chan, K. Englehart, and O. Stavdahl, "Resolving the Limb Position Effect in Myoelectric Pattern Recognition," *IEEE Transactions on Neural Systems and Rehabilitation Engineering*, vol. 19, no. 6, pp. 644–651, 2011.

[9] J. L. Betthauser, C. L. Hunt, L. E. Osborn, R. R. Kaliki, and N. V. Thakor, "Limb-Position Robust Classification of Myoelectric Signals for Prosthesis Control using Sparse Representations," in *38th International Conference of the IEEE Engineering in Medicine and Biology Society*, pp. 6373–6376, 2016.

[10] A. J. Young, L. J. Hargrove, and T. A. Kuiken, "Improving myoelectric pattern recognition robustness to electrode shift by changing interelectrode distance and electrode configuration," *IEEE Transactions on Biomedical Engineering*, vol. 59, no. 3, pp. 645–652, 2012.

[11] M. a. Powell, R. R. Kaliki, and N. V. Thakor, "User training for pattern recognition-based myoelectric prostheses: Improving phantom limb movement consistency and distinguishability," *IEEE Transactions on Neural Systems and Rehabilitation Engineering*, vol. 22, no. 3, pp. 522–532, 2014.

[12] J. He, D. Zhang, N. Jiang, X. Sheng, D. Farina, and X. Zhu, "User adaptation in long-term, open-loop myoelectric training: implications for EMG pattern recognition in prosthesis control," *Journal of Neural Engineering*, vol. 12, no. 4, p. 046005, 2015.

[13] S. Amsuess, P. Goebel, B. Graimann, and D. Farina, "A multi-class proportional myocontrol algorithm for upper limb prosthesis control: Validation in real-life scenarios on amputees," *IEEE Transactions on Neural Systems and Rehabilitation Engineering*, vol. 23, no. 5, pp. 827–836, 2015.

[14] F. V. G. Tenore, A. Ramos, S. Member, A. Fahmy, S. Acharya, S. Member, R. Etienne-cummings, S. Member, and N. V. Thakor, "Decoding of Individuated Finger Movements Using Surface Electromyography," *IEEE Transactions on Biomedical Engineering*, vol. 56, no. 5, pp. 1427–1434, 2009.

[15] L. J. Hargrove, G. Li, K. B. Englehart, and B. S. Hudgins, "Principal components analysis preprocessing for improved classification accuracies in pattern-recognition-based myoelectric control," *IEEE Transactions on Biomedical Engineering*, vol. 56, no. 5, pp. 1407–1414, 2009.

[16] K. Englehart and B. Hudgins, "A robust, real-time control scheme for multifunction myoelectric control.," *IEEE transactions on bio-medical engineering*, vol. 50, no. 7, pp. 848–854, 2003.

[17] K. Englehart, B. Hudgins, and P. Parker, "Multifunction control of prostheses using the myoelectric signal," in *Intelligent Systems and Technologies in Rehabilitation Engineering* (Horia-Nicolai L. Teodorescu and Lakhmi C. Jain, ed.), CRC Press, 2001.

[18] L. J. Hargrove, E. J. Scheme, K. B. Englehart, and B. S. Hudgins, "Multiple binary classifications via linear discriminant analysis for improved controllability of a powered prosthesis," *IEEE Transactions on Neural Systems and Rehabilitation Engineering*, vol. 18, no. 1, pp. 49–57, 2010.

[19] M. Asghari Oskoei and H. Hu, "Myoelectric control systemsA survey," *Biomedical Signal Processing and Control*, vol. 2, no. 4, pp. 275–294, 2007.

[20] A. Phinyomark, F. Quaine, S. Charbonnier, C. Serviere, F. Tarpin-Bernard, and Y. Laurillau, "EMG feature evaluation for improving myoelectric pattern recognition robustness," *Expert Systems with Applications*, vol. 40, no. 12, pp. 4832–4840, 2013.

[21] G. Li, "Electromyography Pattern-Recognition-Based Control of Powered Multifunctional Upper-Limb Prostheses," in *Advances in Applied Electromyography* (P. J. M. (Ed.), ed.), ch. 6, InTech, 2011.

[22] D. Tkach, H. Huang, and T. A. Kuiken, "Study of stability of time-domain features for electromyographic pattern recognition," *Journal of NeuroEngineering and Rehabilitation*, vol. 7, no. 21, pp. 1–13, 2010.

[23] I. Kuzborskij, A. Gijsberts, and B. Caputo, "On the challenge of classifying 52 hand movements from surface electromyography," in *Proceedings of the Annual International Conference of the IEEE Engineering in Medicine and Biology Society, EMBS*, pp. 4931–4937, 2012.

[24] M. F. Lucas, A. Gaufriau, S. Pascual, C. Doncarli, and D. Farina, "Multi-channel surface EMG classification using support vector machines and signal-based wavelet optimization," *Biomedical Signal Processing and Control*, vol. 3, no. 2, pp. 169–174, 2008.

[25] A. D. C. Chan and K. B. Englehart, "Continuous Myoelectric Control for Powered Prostheses Using Hidden Markov Models," *IEEE TRANSACTIONS ON BIOMEDICAL ENGINEERING*, vol. 52, no. 1, pp. 121–124, 2005.

[26] Y. Huang, K. B. Englehart, B. Hudgins, and A. D. C. Chan, "A Gaussian mixture model based classification scheme for myoelectric control of powered upper limb prostheses," *IEEE Transactions on Biomedical Engineering*, vol. 52, no. 11, pp. 1801–1811, 2005.

[27] C. Cipriani, C. Antfolk, M. Controzzi, G. Lundborg, B. Rosen, M. C. Carrozza, and F. Sebelius, "Online Myoelectric Control of a Dexterous Hand Prosthesis by Transradial Amputees," *IEEE Transactions on Neural Systems and Rehabilitation Engineering*, vol. 19, no. 3, pp. 260–270, 2011.

[28] M. Atzori and H. Müller, "Control Capabilities of Myoelectric Robotic Prostheses by Hand Amputees: A Scientific Research and Market Overview," *Frontiers in Neuroscience*, vol. 9, no. 162, 2015.

[29] S. Jain, G. Singhal, R. J. Smith, R. Kaliki, and N. Thakor, "Improving long term myoelectric decoding, using an adaptive classifier with label correction," in *The Fourth IEEE RAS/EMBS International Conference on Biomedical Robotics and Biomechatronics*, (Roma, Italy), pp. 532–537, 2012.

[30] S. Amsuss, P. M. Goebel, N. Jiang, B. Graimann, L. Paredes, and D. Farina, "Self-correcting pattern recognition system of surface EMG signals for upper limb prosthesis control," *IEEE Transactions on Biomedical Engineering*, vol. 61, no. 4, pp. 1167–1176, 2014.

[31] E. Scheme and K. Englehart, "Electromyogram pattern recognition for control of powered upper-limb prostheses: State of the art and challenges for clinical use," *Journal of Rehabilitation Research and Development*, vol. 48, no. 6, pp. 643–660, 2011.

[32] D. Farina, N. Jiang, H. Rehbaum, A. Holobar, B. Graimann, H. Dietl, and O. C. Aszmann, "The extraction of neural information from the surface EMG for the control of upper-limb prostheses: Emerging avenues and challenges," *IEEE Transactions on Neural Systems and Rehabilitation Engineering*, vol. 22, no. 4, pp. 797–809, 2014.

[33] J. Liu, X. Sheng, D. Zhang, N. Jiang, and X. Zhu, "Towards Zero Retraining for Myoelectric Control Based on Common Model Component Analysis," *IEEE Transactions on Neural Systems and Rehabilitation Engineering*, vol. 24, no. 4, pp. 444–454, 2016.

[34] J. W. Sensinger, B. A. Lock, and T. A. Kuiken, "Adaptive pattern recognition of myoelectric signals: Exploration of conceptual framework and practical algorithms," *IEEE Transactions on Neural Systems and Rehabilitation Engineering*, vol. 17, no. 3, pp. 270–278, 2009.

[35] D. Nishikawa, W. Yu, H. Yokoi, and Y. Kakazu, "On-Line Learning Method for EMG Prosthetic Hand Controlling," *Electronics and Communications in Japan*, vol. 84, no. 10, pp. 35–46, 2001.

[36] D. Nishikawa, W. Yu, H. Yokoi, and Y. Kakazu, "EMG prosthetic hand controller discriminating ten motions using\nreal-time learning method," *Proceedings 1999 IEEE/RSJ International Conference on Intelligent Robots and Systems. Human and Environment Friendly Robots with High Intelligence and Emotional Quotients (Cat. No.99CH36289)*, vol. 3, pp. 0–5, 1999.

[37] X. Zhang, H. Huang, and Q. Yang, "Real-time implementation of a self-recovery EMG pattern recognition interface for artificial arms," *Proceedings of the Annual International Conference of the IEEE Engineering in Medicine and Biology Society, EMBS*, pp. 5926–5929, 2013.

[38] X. Chen, D. Zhang, and X. Zhu, "Application of a self-enhancing classification method to electromyography pattern recognition for multifunctional prosthesis control.," *Journal of neuroengineering and rehabilitation*, vol. 10, no. 1, p. 44, 2013.

[39] J. Liu, "Adaptive myoelectric pattern recognition toward improved multifunctional prosthesis control," *Medical Engineering and Physics*, vol. 37, no. 4, pp. 424–430, 2015.

[40] O. Fukuda, T. Tsuji, M. Kaneko, and A. Otsuka, "A human-assisting manipulator teleoperated by EMG signals and arm motions," *IEEE Transactions on Robotics and Automation*, vol. 19, no. 2, pp. 210–222, 2003.

[41] N. Bu, O. Fukuda, and T. Tsuji, "EMG-Based Motion Discrimination Using a Novel Recurrent Neural Network," *Journal of Intelligent Information Systems*, vol. 21, no. 2, pp. 113–126, 2003.

[42] O. Fukuda, T. Tsuji, A. Ohtsuka, and M. Kaneko, "EMG-based Human-Robot Interface for Rehabilitation Aid," in *IEEE International Conference on Robotics and Automation*, no. May, pp. 3492–3497, 1998.

[43] O. Fukuda, T. Tsuji, A. Otsuka, and M. Kaneko, "A Human Supporting Manipulator Using Neural Network and Its Clinical Application for Forearm Amputation," in *Third International Conference on Knowledge-Based Intelligent Information Engineering Systems*, 1999.

[44] O. Fukuda, T. Tsuji, H. Shigeyoshi, and M. Kaneko, "An EMG controlled human supporting robot using neural network," in *Proceedings 1999 IEEE/RSJ International Conference on Intelligent Robots and Systems.*, vol. 3, pp. 1586–1591, 1999.

[45] T. Tsuji, R. O. Fukuda, M. Kaneko, and K. Ito, "Pattern classification of time-series EMG signals using neural networks," *International Journal of Adaptive Control and Signal Processing*, vol. 14, no. 8, pp. 829–848, 2000.

[46] U. Baspinar, H. S. Varol, and V. Y. Senyurek, "Performance comparison of artificial neural network and gaussian mixture model in classifying hand motions by using sEMG signals," *Biocybernetics and Biomedical Engineering*, vol. 33, no. 1, pp. 33–45, 2013.

[47] B. Hudgins, P. Parker, and R. N. Scott, "A New Strategy for Multifunction Myoelectric Control," *IEEE Transactions on Biomedical Engineering*, vol. 40, no. 1, pp. 82–94, 1993.

[48] P. Gallant, E. Morin, and L. Peppard, "Feature-based classification of myoelectric signals using artificial neural networks," *Medical and Biological Engineering and Computing*, vol. 36, no. 4, pp. 485–489, 1998.

[49] F. E. R. Mattioli, E. a. Lamounier, A. Cardoso, A. B. Soares, and A. O. Andrade, "Classification of EMG signals using artificial neural networks for virtual hand prosthesis control.," in *33rd Annual International Conference of the IEEE Engineering in Medicine and Biology Society.*, vol. 2011, pp. 7254–7, 2011.

[50] R. Kato, T. Fujita, H. Yokoi, and T. Arai, "Adaptable EMG prosthetic hand using on-line learning method -Investigation of mutual adaptation between human and adaptable machine," in *The 15th IEEE International Symposium on Robot and Human Interactive Communication (RO-MAN06)*, pp. 599–604, 2006.

[51] Z. Jingdong, X. Zongwu, J. Li, C. Hegao, L. Hong, and H. Gerd, "EMG control for a five-fingered underactuated prosthetic hand based on wavelet transform and sample entropy," in *IEEE/RSJ International Conference on Intelligent Robots and Systems*, no. 50435040, pp. 3215–3220, 2006.

[52] D. F. Stegeman, J. H. Blok, H. J. Hermens, and K. Roeleveld, "Surface EMG models: properties and applications," *Journal of Electromyography and Kinesiology*, vol. 10, pp. 313–326, aug 2000.

[53] J. Rodriguez-falces, J. Navallas, and A. Malanda, "EMG Modeling," in *Computational Intelligence in Electromyography Analysis A Perspective on Current Applications and Future Challenges*, ch. 1, pp. 3–36, InTech, 2012.

[54] K. C. Mcgill, "Surface electromyogram signal modeling," *Medical & biological engineering & computing*, vol. 42, no. 4, pp. 446–454, 2004.

[55] R. Plonsey, "The active fiber in a volume conductor.," *IEEE Transactions on Biomedical Engineering*, vol. 21, no. 5, pp. 371–81, 1974.

[56] R. Plonsey, "Action Potential Sources and Their Volume Conductor Fields," *Proceedings of the IEEE*, vol. 65, no. 5, pp. 601–611, 1977.

[57] S. D. Nandedkar, D. B. Sanders, E. V. Stalberg, and S. Andreassen, "Simulation of concentric needle EMG motor unit action potentials," *Muscle & Nerve*, vol. 6, no. February, p. 562, 1984.

[58] S. D. Nandedkar and E. Stlberg, "Simulation of single muscle fibre action potentials," *Medical and Biological Engineering and Computing*, vol. 21, no. 2, pp. 158–165, 1983.

[59] R. A. Conwit, D. Stashuk, B. Tracy, M. McHugh, W. F. Brown, and E. J. Metter, "The relationship of motor unit size, firing rate and force," *Clinical Neurophysiology*, vol. 110, no. 7, pp. 1270–1275, 1999.

[60] R. Merletti, L. Lo Conte, E. Avignone, and P. Guglielminotti, "Modeling of surface myoelectric signals - Part I: Model implementation," *IEEE Transactions on Biomedical Engineering*, vol. 46, no. 7, pp. 810–820, 1999.

[61] J. Duchêne and J. Y. Hogrel, "A model of EMG generation," *IEEE Transactions on Biomedical Engineering*, vol. 47, no. 2, pp. 192–201, 2000.

[62] C. J. de Luca, "Physiology and Mathematics of Myoelectric Signals," *IEEE Transactions on Biomedical Engineering*, vol. BME-26, no. 6, pp. 313–325, 1979.

[63] P. Konrad, "The abc of emg," *A practical introduction to kinesiological ...*, no. April, pp. 1–60, 2005.

[64] D. Stashuk, "EMG signal decomposition: how can it be accomplished and used?," *Journal of Electromyography and Kinesiology*, vol. 11, pp. 151–173, jun 2001.

[65] T. Adel and D. Stashuk, "Clinical Quantitative Electromyography," *IN-TECH*, 2013.

[66] N. Dimitrova and G. Dimitrov, "Electromyography (EMG) Modeling," in *Wiley Encyclopedia of Biomedical Engineering*, John Wiley & Sons, Inc., 2006.

[67] C. J. De Luca, "Physiology and mathematics of myoelectric signals.," *IEEE transactions on bio-medical engineering*, vol. 26, no. 6, pp. 313–325, 1979.

[68] W. Wang, A. D. Stefano, and R. Allen, "A simulation model of the surface EMG signal for analysis of muscle activity during the gait cycle," *Computers in Biology and Medicine*, vol. 36, no. 6, pp. 601–618, 2006.

[69] L. Du, F. Zhang, H. He, and H. Huang, "Improving the performance of a neural-machine interface for prosthetic legs using adaptive pattern classifiers," *Proceedings of the Annual International Conference of the IEEE Engineering in Medicine and Biology Society, EMBS*, pp. 1571–1574, 2013.

[70] Y. Zhang, Z. Wang, and Z. Zhang, "Comparison of Online Adaptive Learning Algorithms for Myoelectric Hand Control," pp. 69–75, 2016.

[71] P. Kaufmann, K. Englehart, and M. Platzner, "Fluctuating EMG Signals : Investigating Long-term Effects of Pattern Matching Algorithms," in *32nd Annual International Conference of the IEEE EMBS*, (Buenos Aires), pp. 6357–6360, 2010.

[72] L. H. Smith, L. J. Hargrove, B. A. Lock, and T. A. Kuiken, "Determining the optimal window length for pattern recognition-based myoelectric control: Balancing the competing effects of classification error and controller delay," *IEEE Transactions on Neural Systems and Rehabilitation Engineering*, vol. 19, no. 2, pp. 186–192, 2011.

[73] E. Alpaydn, *Introduction to Machine Learning Second Edition.* Massachusetts London, England: The MIT Press Cambridge, 2nd ed., 2010.

NEURAL NETWORK-BASED ADAPTIVE MYOELECTRIC SIGNAL CLASSIFICATION VIA UTILIZATION OF ENTROPY HISTORY